R&D for ATLAS planar pixels for HL-LHC

Marco Bomben - LPNHE

Outline

- Introduction
- The LHC upgrade
- The ATLAS upgrade
- The R&D for a new Inner Detector: the ATLAS Upgrade Planar Pixel Sensor
- Conclusions

INTRODUCTION

LHC

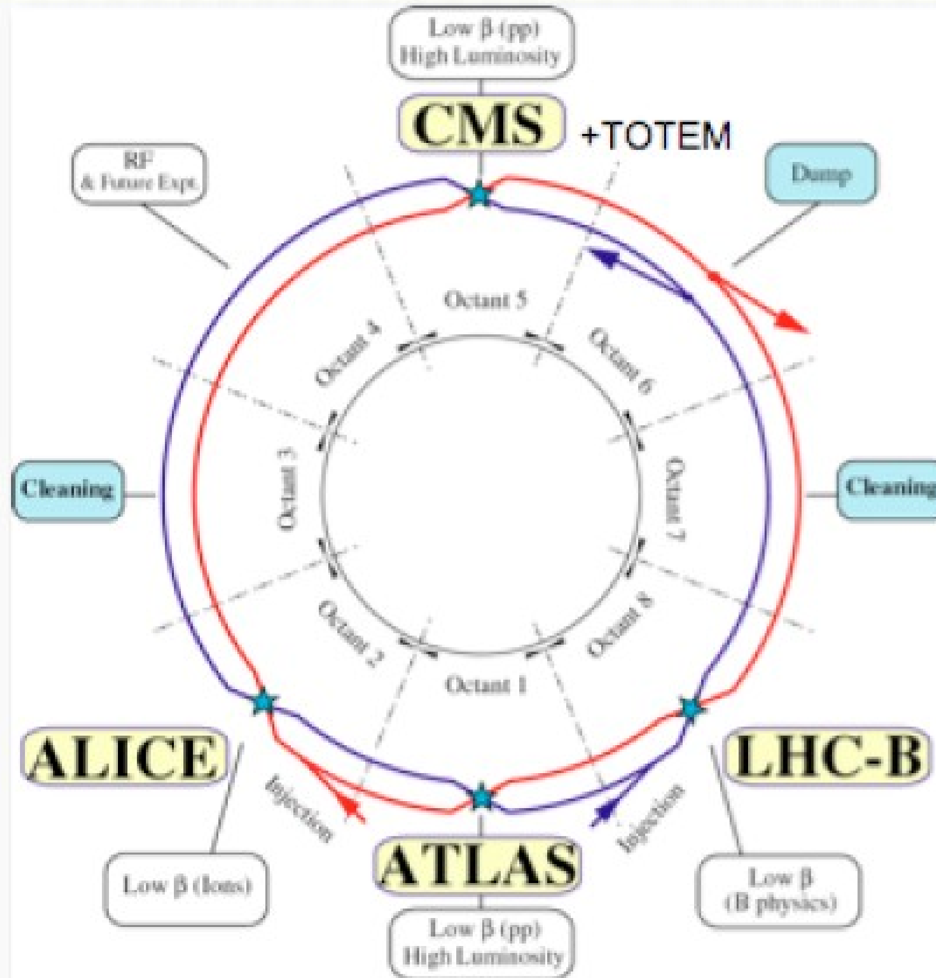

- 1232 superconducting dipoles
  - 15m long at 1.9 K, B=8.33 T
  - Inner coil diameter = 56 mm

- beam-energy 7 TeV (7x TEVATRON)
- Luminosity 10^{34} $cm^{-2}s^{-1}$ (>100x TEVATRON)
- Bunch spacing 24.95 ns
- Particles/bunch 1.1 10^{11}
- Stored E/beam 350 MJ ~ 80kg of TNT

- Also : Lead Ions operation
  - Energy/nucleon 2.76 TeV / u
  - Total initial lumi 10^{27} cm^{-2} s^{-1}

- 8 independent sectors
  - Challenge for control, powering
- 10 GJ stored in magnets
- Warm insertion regions for beam dump, cleaning, acceleration

ATLAS

Muon Spectrometer ($|\eta|<2.7$) : air-core toroids with gas-based muon chambers
Muon trigger and measurement with momentum resolution < 10% up to E_μ ~ 1 TeV

Length : ~ 46 m
Radius : ~ 12 m
Weight : ~ 7000 tons
~10^8 electronic channels
3000 km of cables

3-level trigger reducing the rate from 40 MHz to ~200 Hz

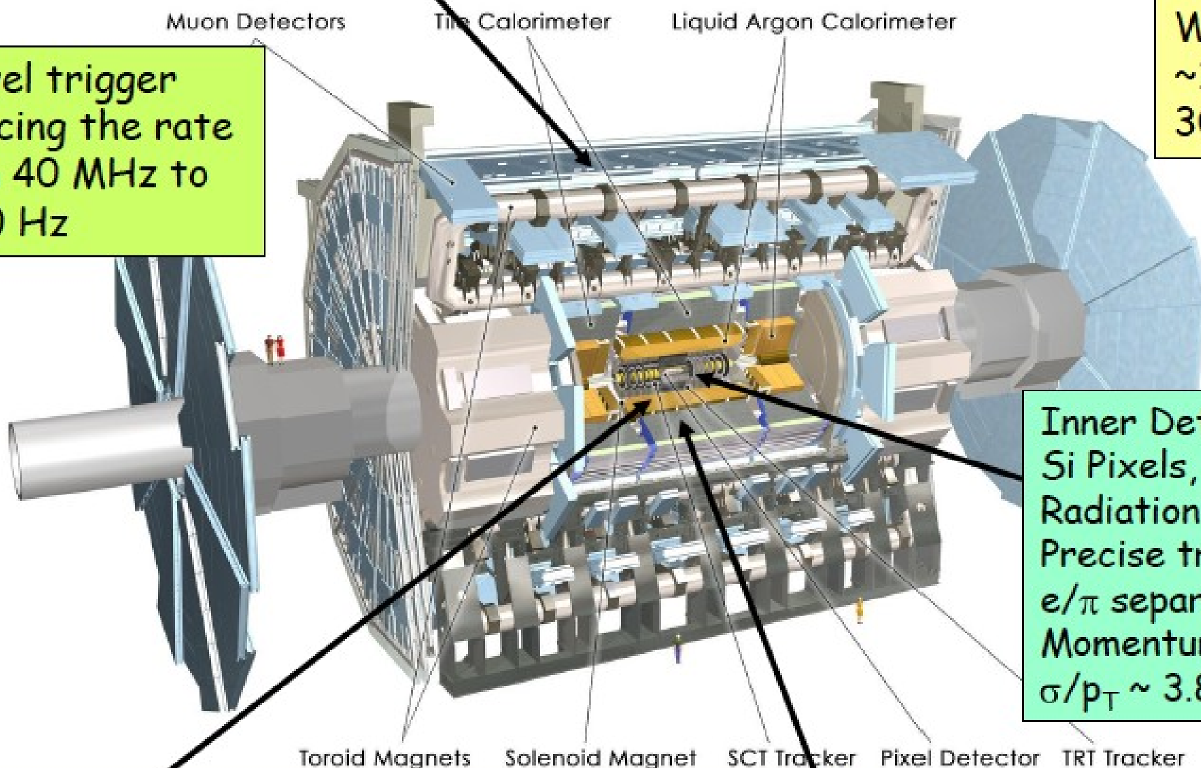

Inner Detector ($|\eta|<2.5$, B=2T):
Si Pixels, Si strips, Transition Radiation detector (straws)
Precise tracking and vertexing, e/π separation
Momentum resolution:
$\sigma/p_T \sim 3.8\times10^{-4}\, p_T(\mathrm{GeV}) \oplus 0.015$

EM calorimeter: Pb-LAr Accordion
e/γ trigger, identification and measurement
E-resolution: $\sigma/E \sim 10\%/\sqrt{E}$

HAD calorimetry ($|\eta|<5$): segmentation, hermeticity
Fe/scintillator Tiles (central), Cu/W-LAr (fwd)
Trigger and measurement of jets and missing E_T
E-resolution: $\sigma/E \sim 50\%/\sqrt{E} \oplus 0.03$

ATLAS status and highlights, ICHEP, 26-7-2010

ATLAS performance

Peak luminosity seen by ATLAS:
~ 3.6 x10^{33} cm^{-2} s^{-1}

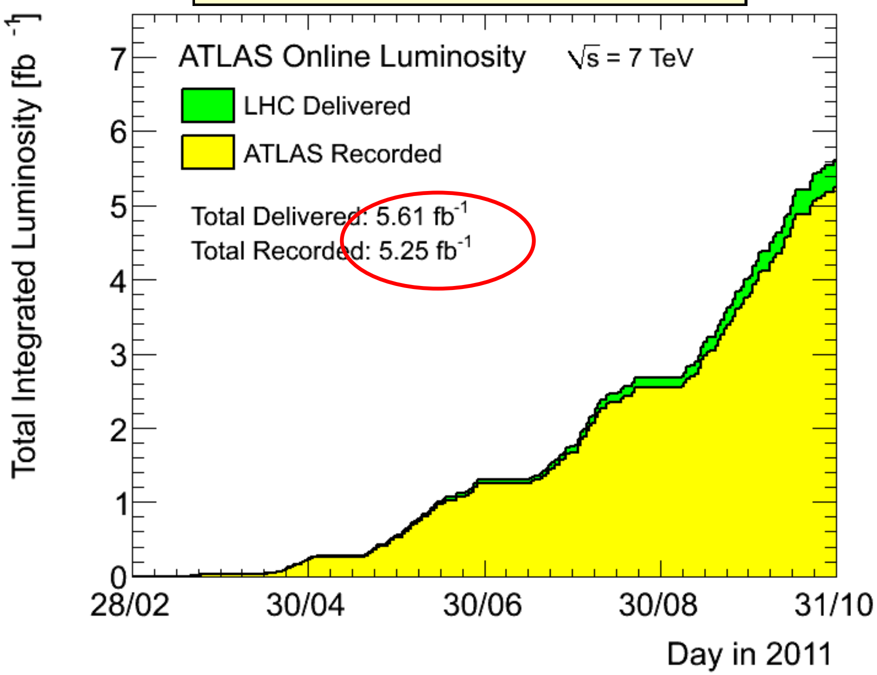

Price to pay for the high luminosity: larger-than-expected pile-up

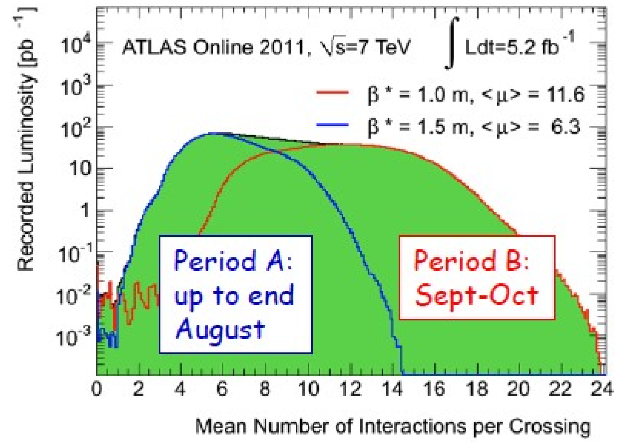

Event with 20 reconstructed vertices (ellipses have 20 σ size for visibility reasons)

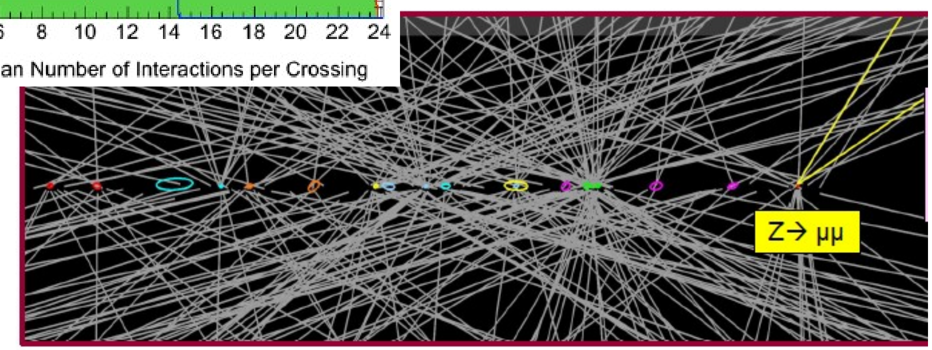

Fraction of non-operational detector channels: (depends on the sub-detector) — few permil to 3.5%

Data-taking efficiency = (recorded lumi)/(delivered lumi): ~ 93.5%

Good-quality data fraction, used for analysis : (depends on the analysis) — 90-96%

LHC Upgrade

LHC in the high lumi area

- The LHC is a discovery machine built to study:
  - → **The ElectroWeak Symmetry Breaking mechanism**
  - → **The shortcomings of the Standard Model**
- The discovery potential of the LHC can be enhanced by increasing its luminosity
- Infact, **whatever is discovered**, we'll want, at least, to:
  - → **Improve the measurement of its properties (masses, couplings, etc)**
  - → **Test further predictions of the theories put forward to explain it**

LHC schedule

Caveat: this schedule spans decades

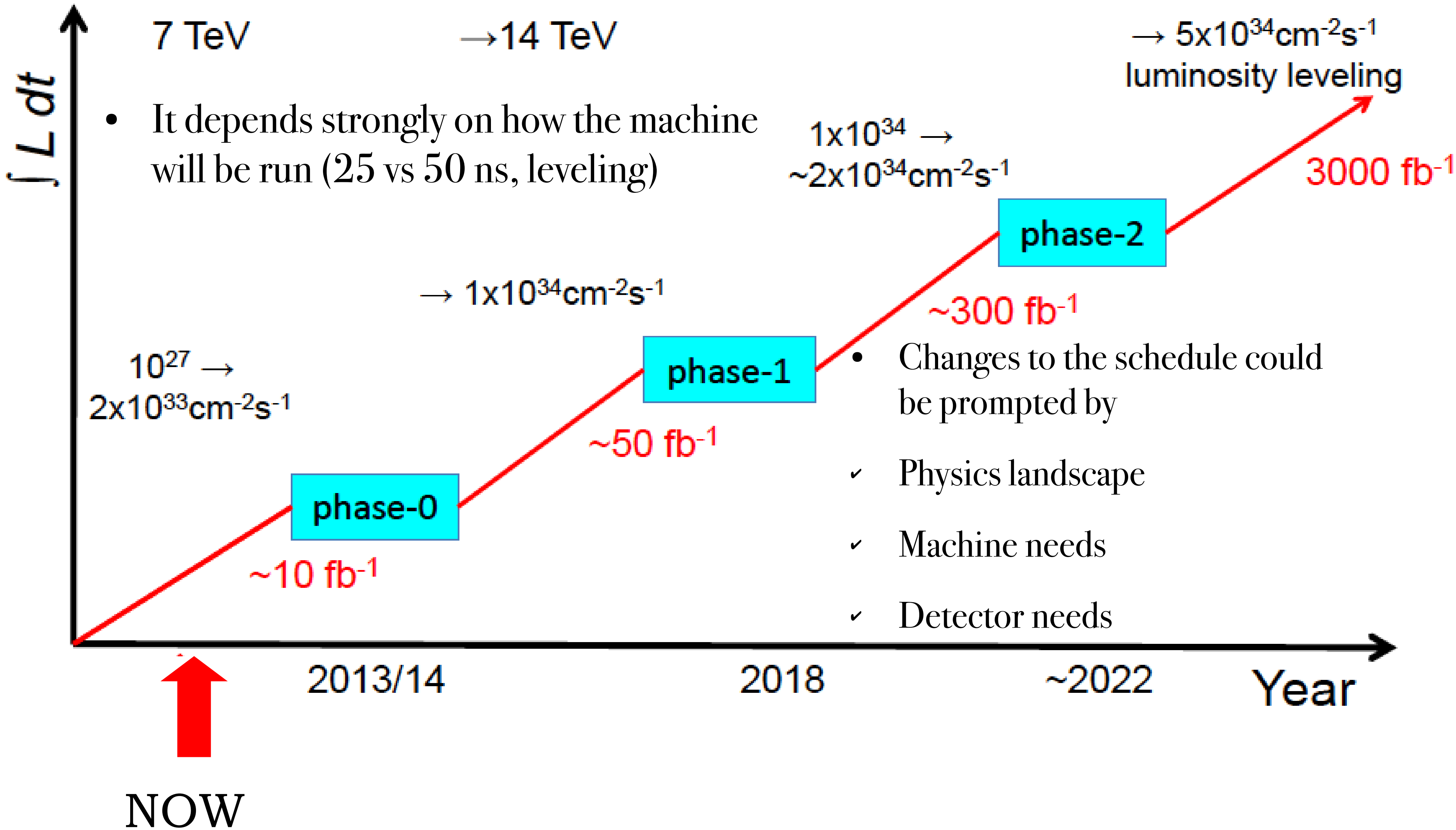

- It depends strongly on how the machine will be run (25 vs 50 ns, leveling)

- Changes to the schedule could be prompted by
  - ✓ Physics landscape
  - ✓ Machine needs
  - ✓ Detector needs

ATLAS upgrade NOW

- Why working now for the phase-2 upgrade?

➔ Everybody who took part to the design of an experiment knows that it takes several years (the construction and installation itself is typically 5-6 years, after the R&D and design phase is finished). Time flows fast!

- LHC will not be the same between now and 2020.
  Radical improvements with respect to the initial detector ("Phase I upgrade")

High-luminosity implications

- Effects due to peak luminosity:
  - High event rate and pile-up
  - Increased occupancy

➔ **Higher granularity sensors**

➔ **Faster electronics**

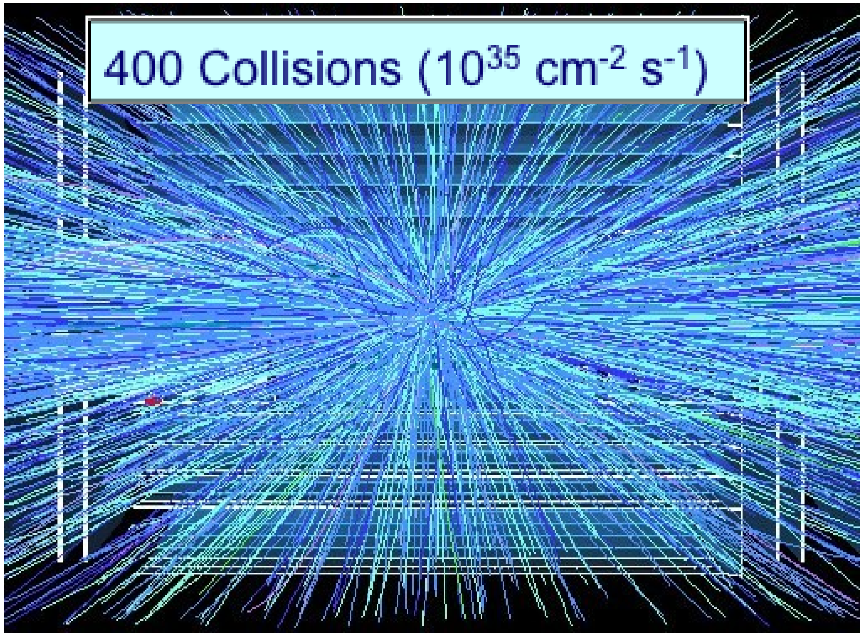

- Effects due to integrated lum.:
  - Increase in leakage current
  - Change in operational voltage
  - Reduced charge collection

➔ **Rad-hard components**

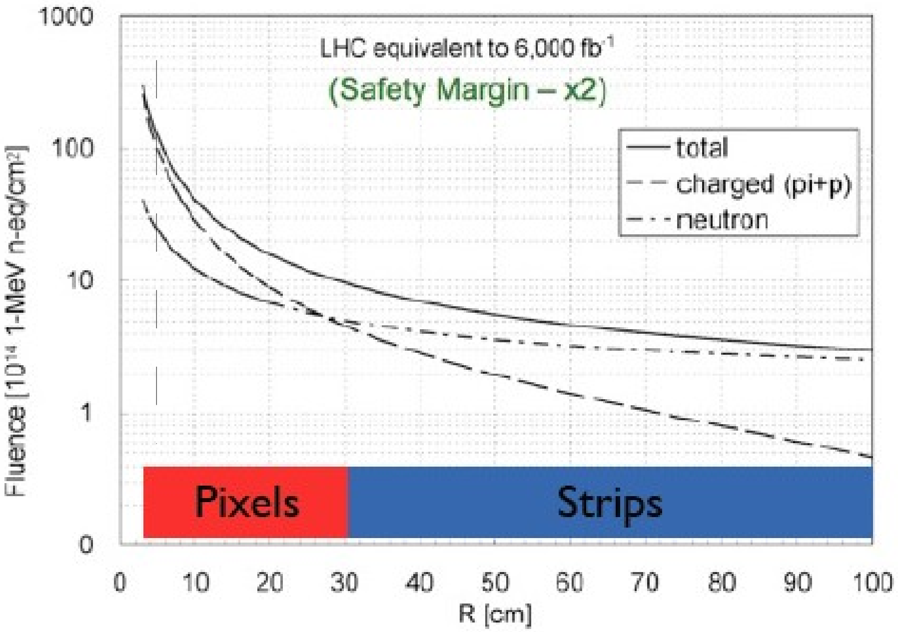

Macroscopic radiation effects

Change of leakage current
- can be helped with cooling

Change of the full depletion voltage V_{dep} (effective doping concentration N_{eff}).
- every p-n-junction has a finite breakdown voltage

Decrease of the charge collection efficiency
- limited by partial depletion, trapping, type inversion

Change of the leakage current:

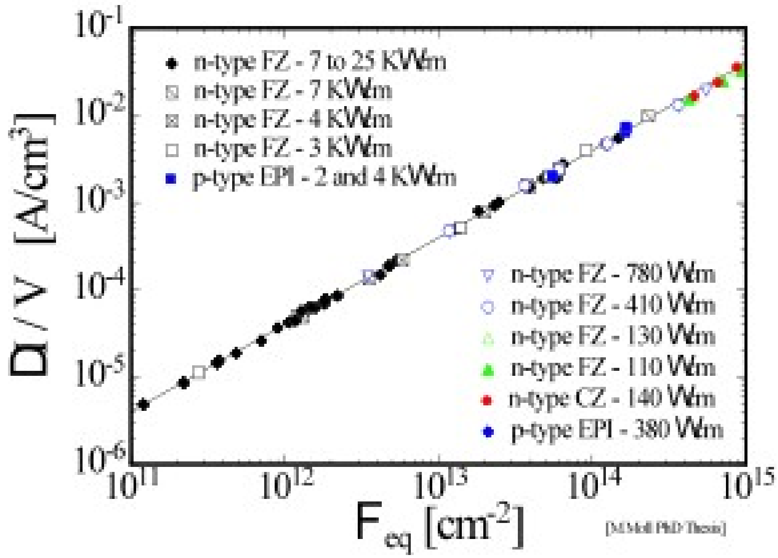

Evolution of the N_{eff} for n-type initial doping:

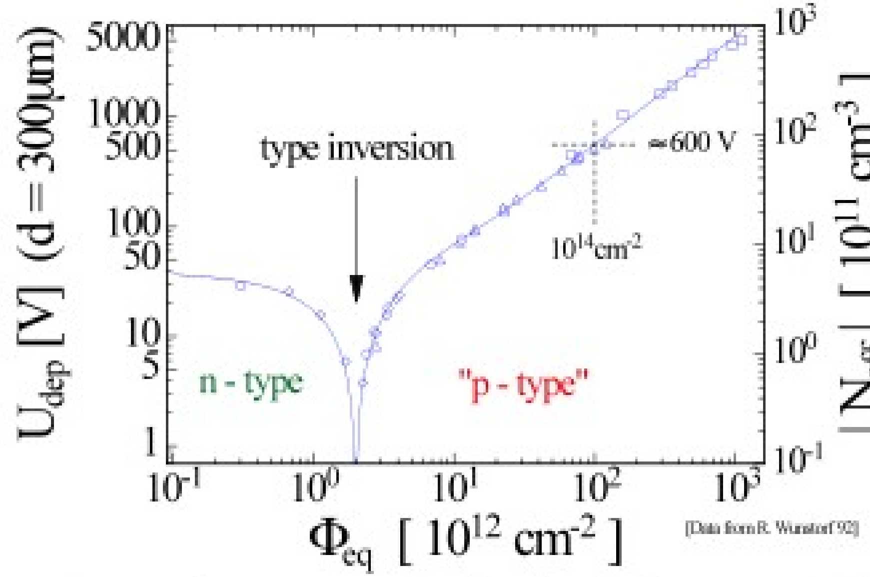

Panja Luukka, The Fifth International Forum on Advanced Material Science and Technology (IFAMST5 2006)

Microscopic damage effects

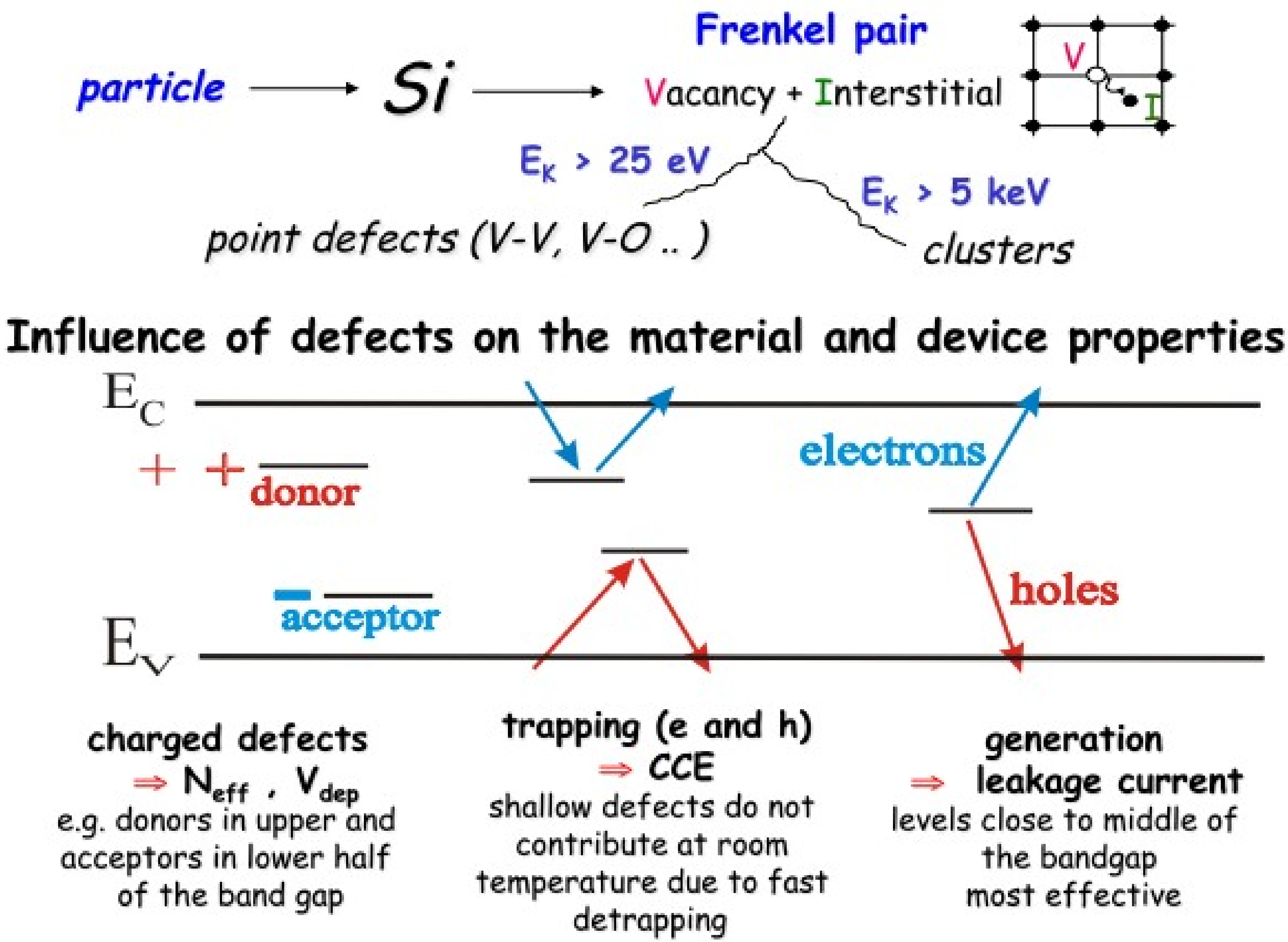

Panja Luukka, The Fifth International Forum on Advanced Material Science and Technology (IFAMST5 2006)

The Pixel Upgrade

The ATLAS Inner Detector

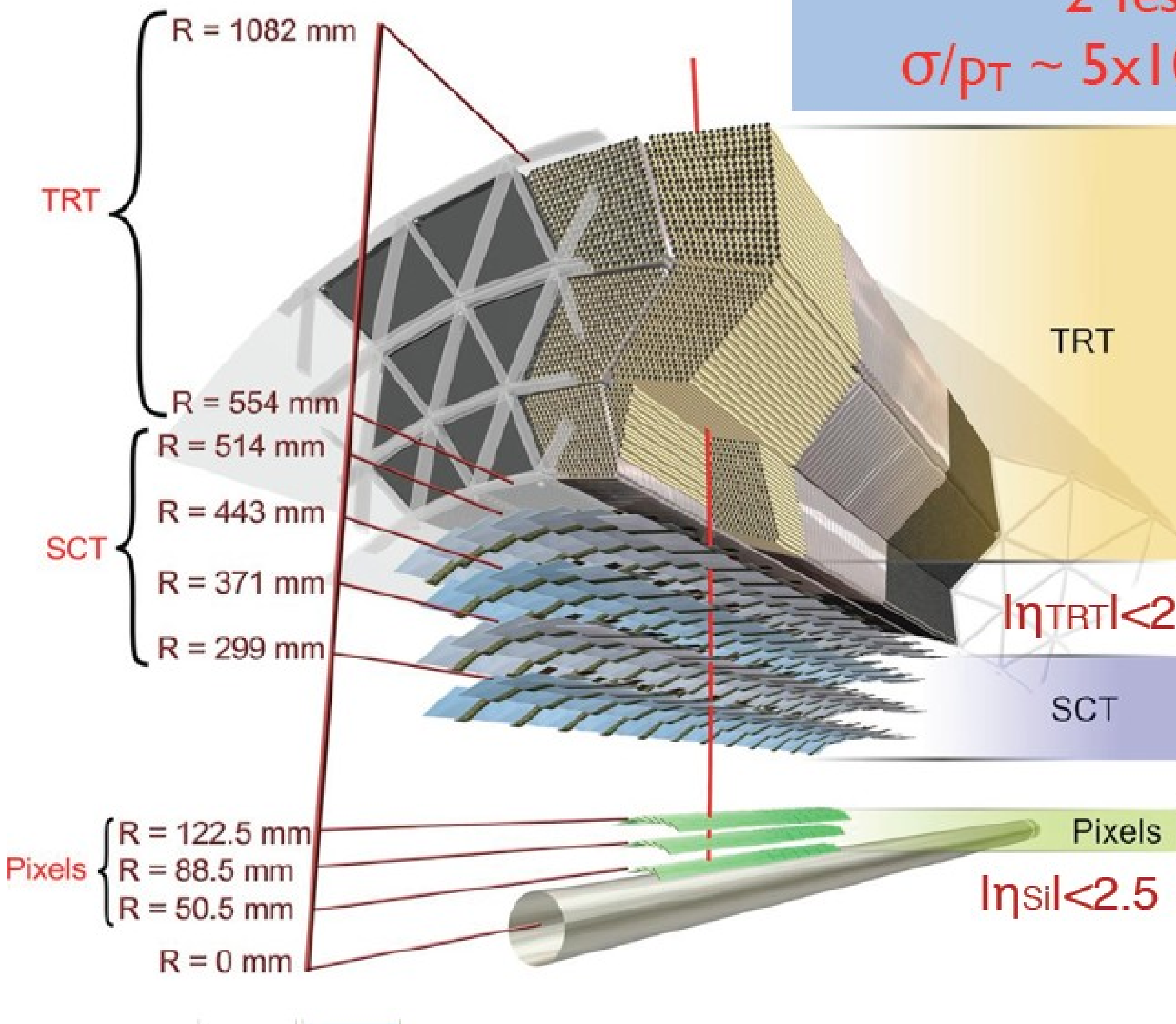

2 Tesla Solenoid

$\sigma/p_T \sim 5\times10^{-4}\ p_T/\mathrm{GeV} \oplus 0.01$

Transition Radiation Tracker (TRT) (350k channels) with e/π separation

SemiConductor Tracker (SCT) ~6M silicon strips

Pixels: 80M channels

The current ATLAS pixels

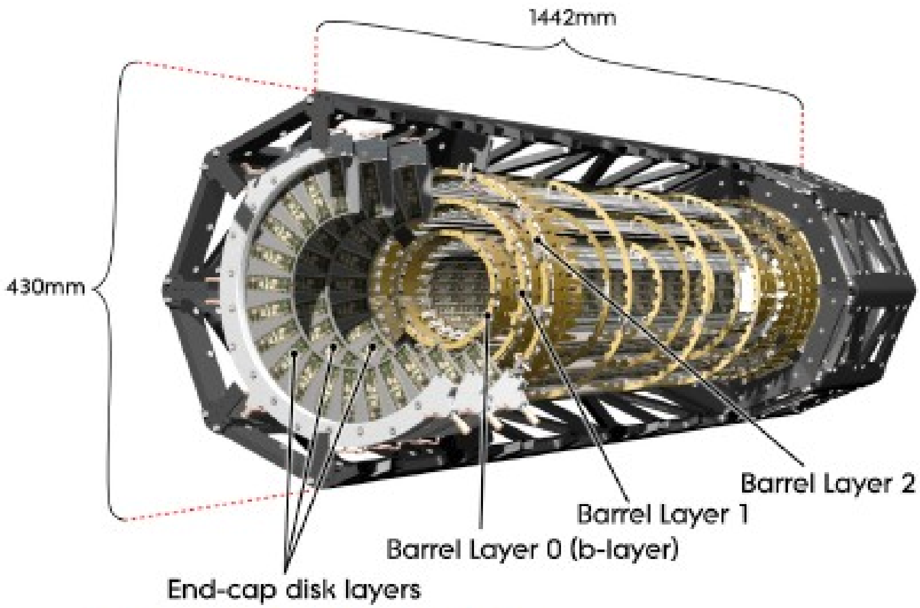

- ATLAS Pixel Detector
  - 3 barrels + 3 forward/backwarc disks
  - 112 stave and 4 sectors
  - 1744 modules
  - 80 million channels

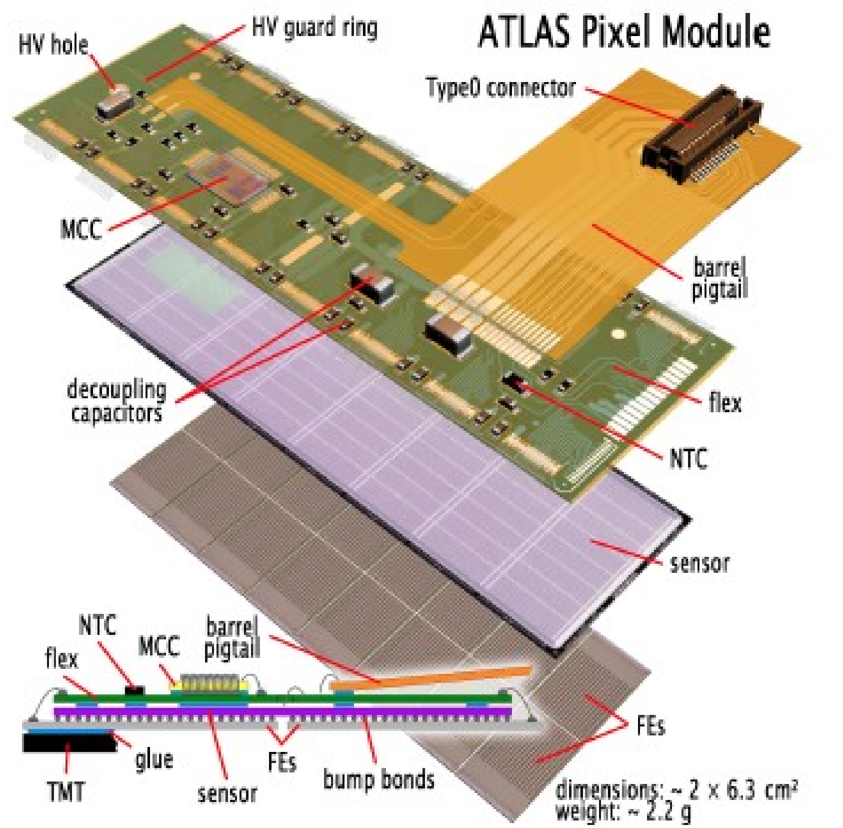

- **ATLAS Pixel Module**
  - 16 front-end chips (FE-I3) module with a Module Controller Chip (MCC)
  - 46080 R/O channels 50 μm x 400 μm (50 μm x 600 μm for edge pixel columns between neighbour FE-I3 chips)
  - Planar n-in-n DOFZ silicon sensors, 250um tick
  - Designed for 1 x 10^{15} 1MeV fluence and 50 Mrad
  - Optolink R/O: 40÷80 Mb/link

IPRD10, Siena 9.6.2010 - Alessandro La Rosa (CERN)

The ATLAS pixel sensor

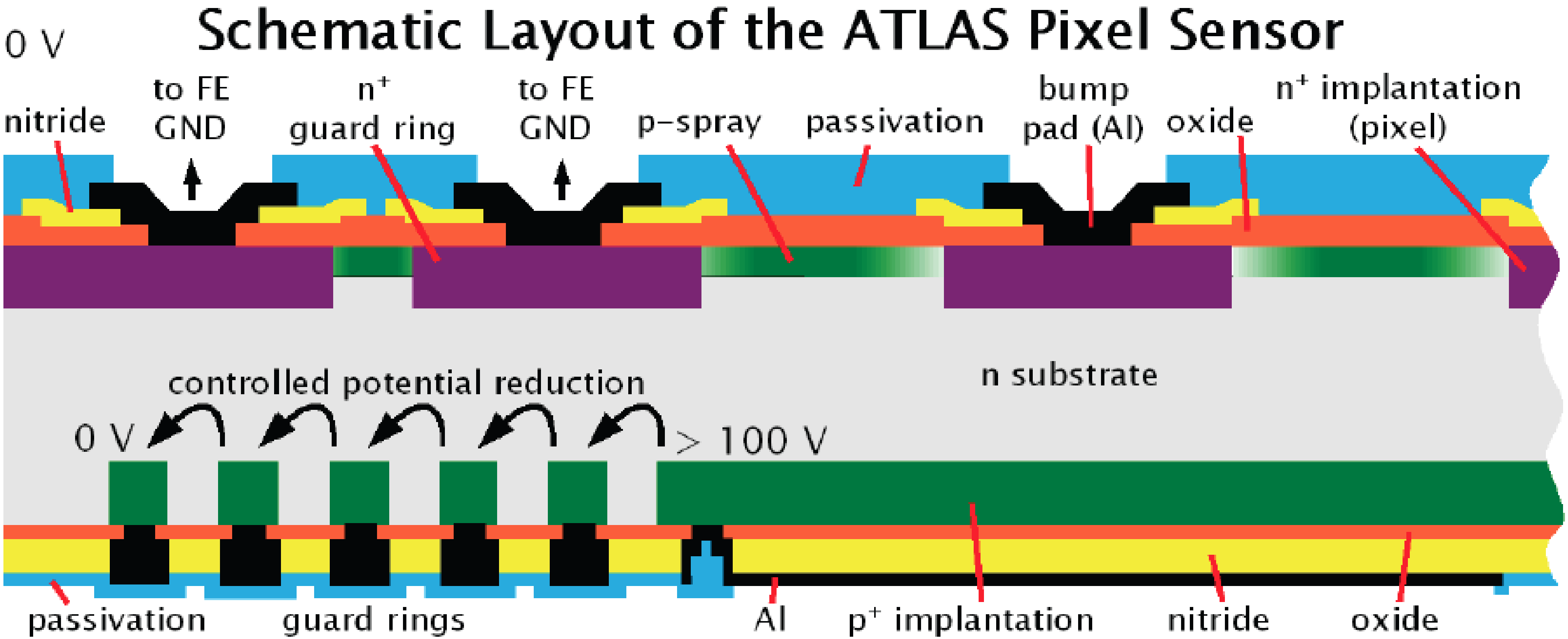

ATLAS ID upgrade

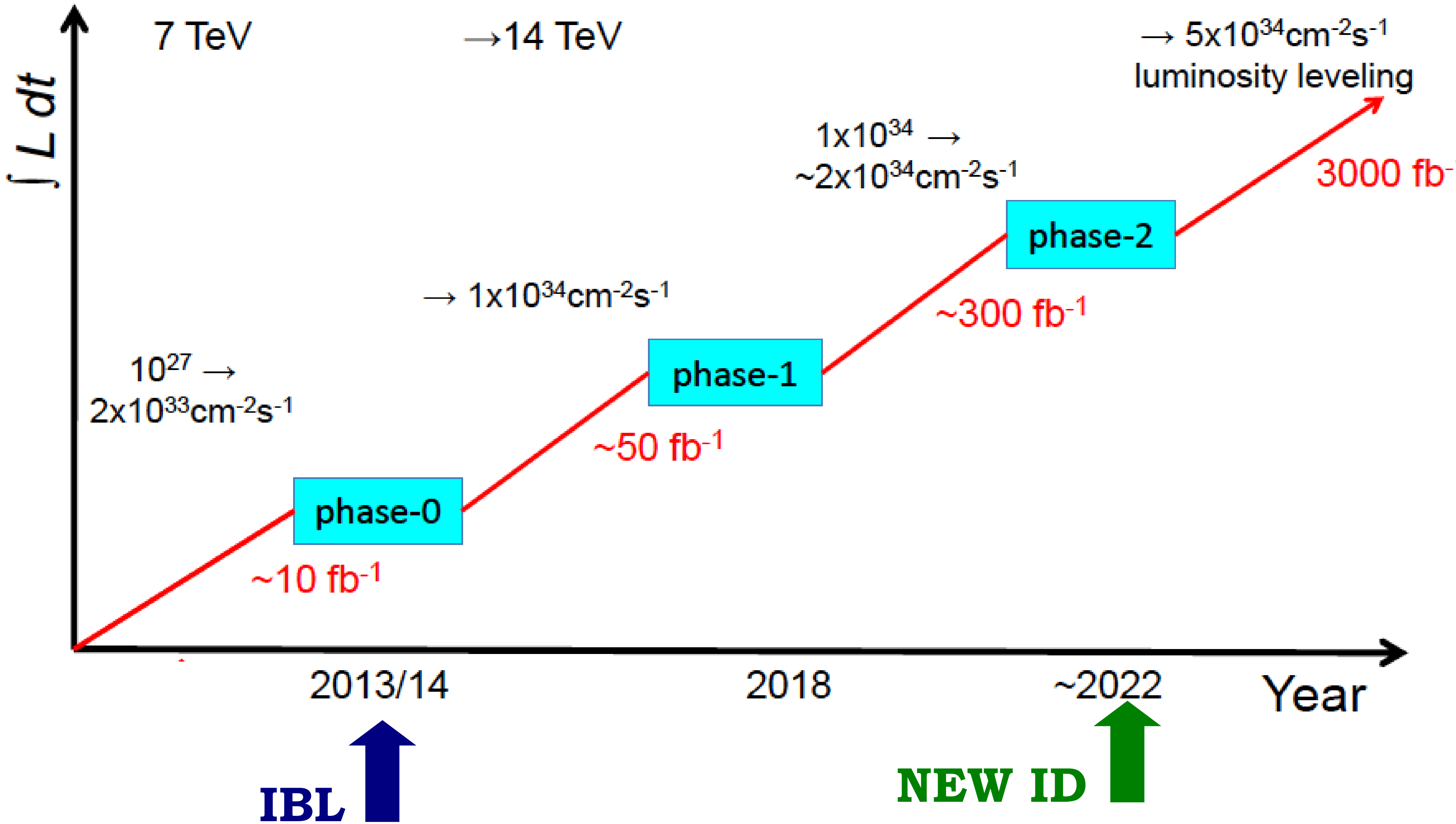

The Insertable B-Layer

A 4^{th} pixel Layer: IBL

- Adding a 4^{th} pixel layer inside the present B-Layer: the insertable B-Layer

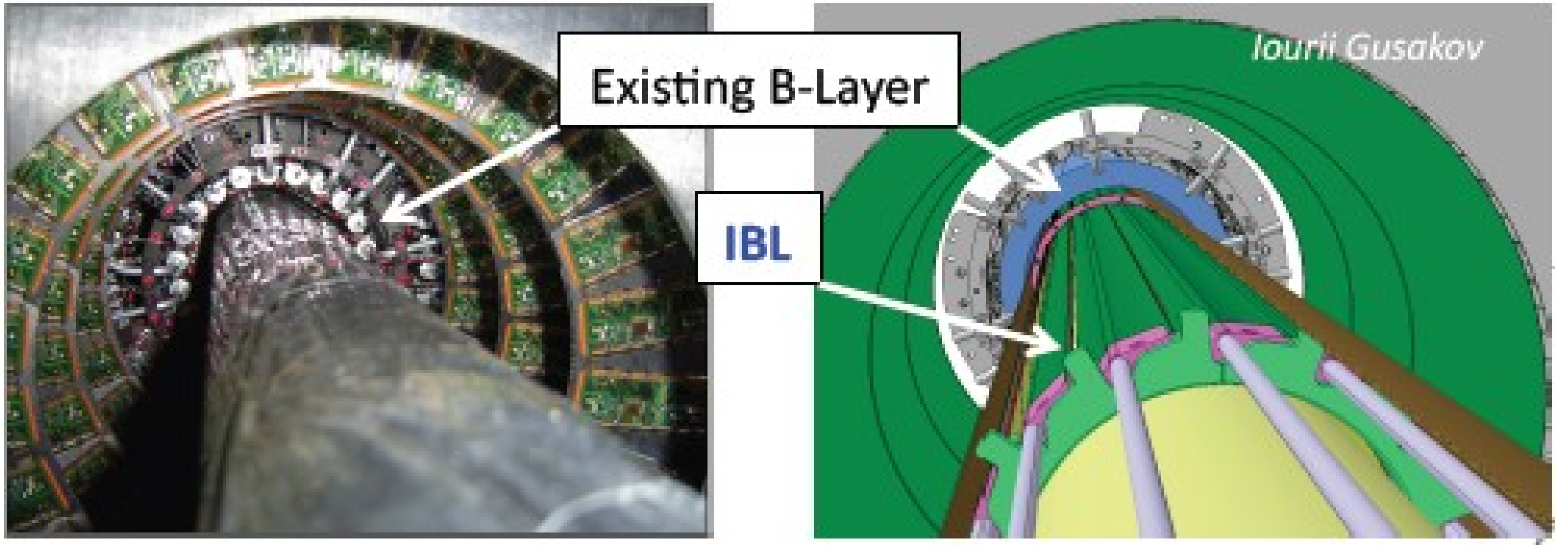

- To improve the performance of the existing system
- To maintain performance of existing system when present B-layer starts degrading

Scheduled for 2013

IBL

- Operation:
  - 14 Staves @ R=3.3 cm, |η|<2.5, 0.2 m^2
  - No overlap on Z due to space restriction
  - Operate at -15 C, CO_2 cooling

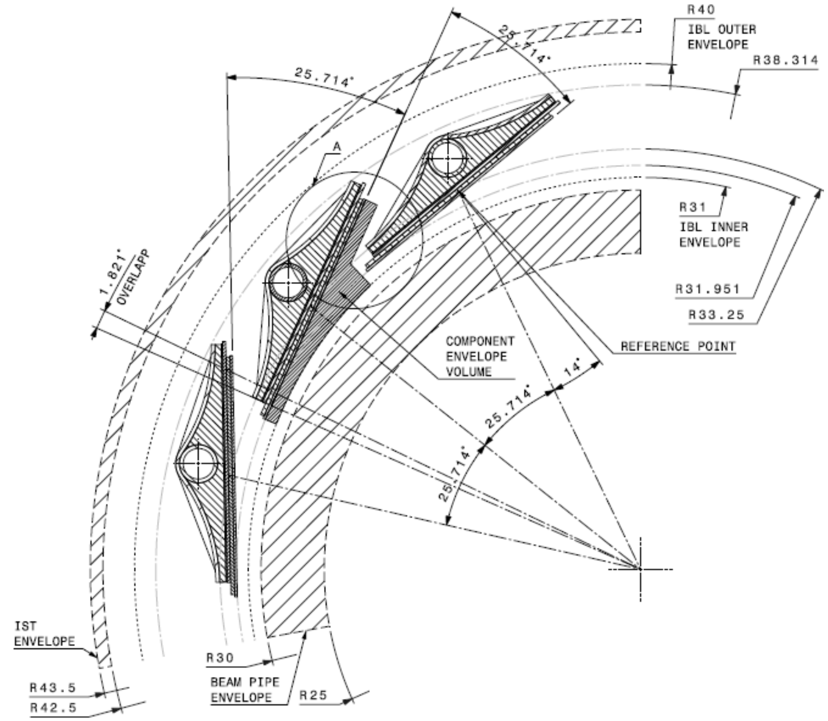

- Front-end/Sensor Design:
  - NIEL dose = 5x10^{15} n_{eq} cm^{-2} (w/ safety factor)
  - Ionizing dose ≥ 250 Mrad
  - Small dead area (slim/active edge)
  - Max sensor power < 200 mW/cm^2 @ -15 C
  - Max bias voltage: 1000V

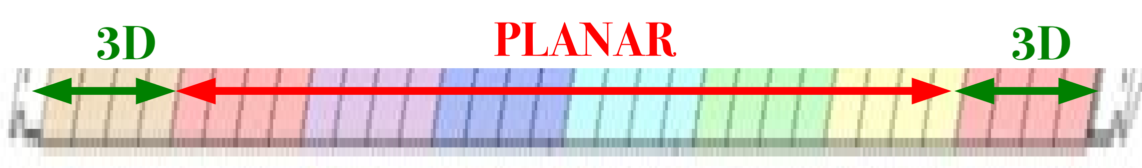

- Sensor Technology
  - Planar n-on-n and 3D double sided being considered
  - 75% Planar and 25% 3D sensor layout

IBL: Font End Chip: FE-I4 (“A”)

- Biggest chip in HEP to date
- Higher active fraction (x6)
  (than ATLAS predecessor)
- Local memory cells (bus activity only on readout) → Lower power
- Higher data rate
- More radiation hard (130nm technology)

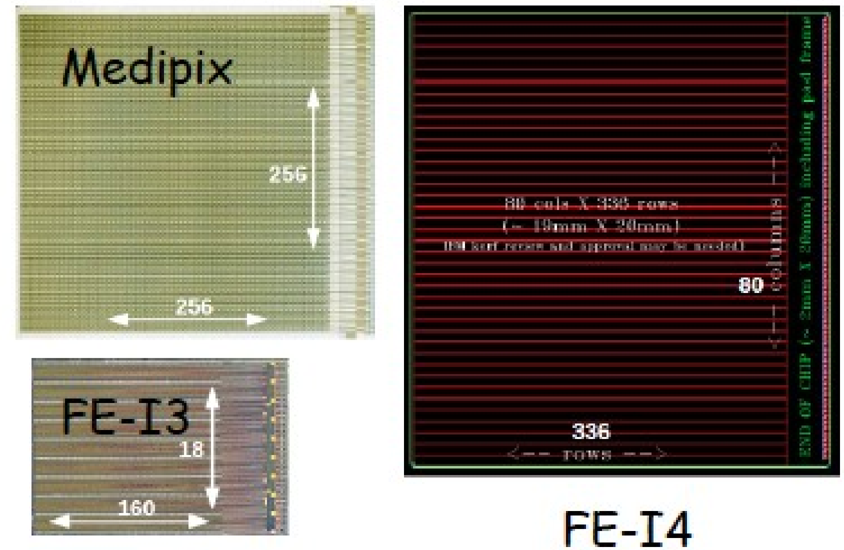

Pixel array	80x336
Chip size (mm2)	20.2x19.0
Active fraction (%)	89
Analog/Digital current (uA/pix)	10/10
Analog/Digital voltage (V)	1.5/1.2
LVDS output (Mb/s)	160
Pixel sixe (um2)	50 x 250
ToT Resolution	4-bit

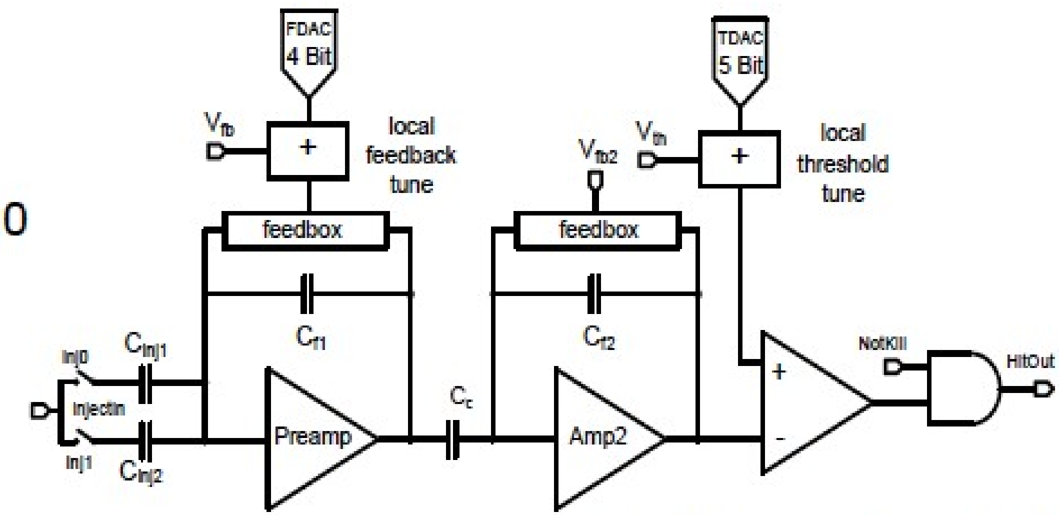

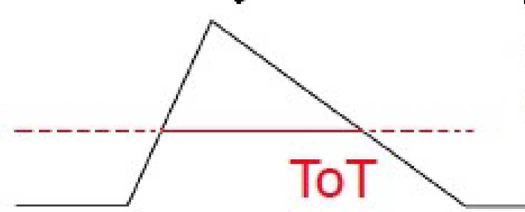

- Pixel above threshold
- Time over threshold (~collected charge)

Beyond 2020:
The Planar Pixel Sensor Project

Sensor options for Phase 2

PLANAR

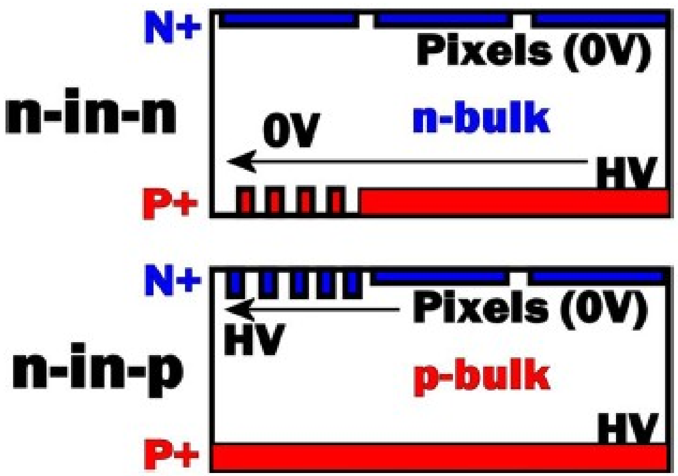

- More details in the next slides

DIAMOND

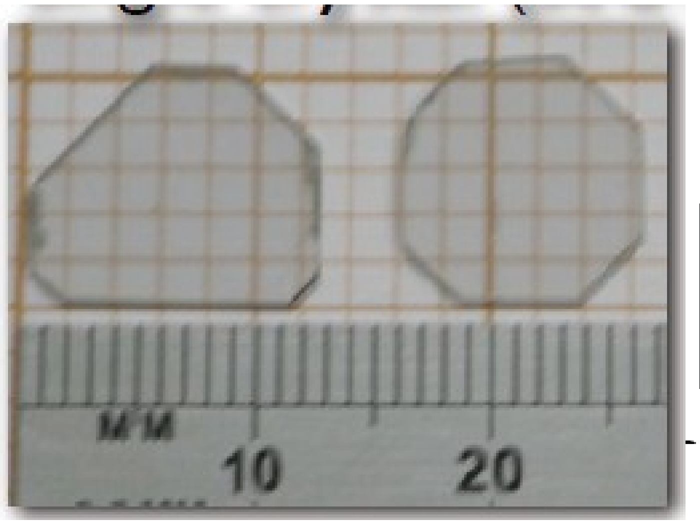

- Very low noise
- No cooling
- No doping needed
- Low capacitance
- Very high BD field
- Expensive
- Difficult to realize large sample of single crystal sensors

3D

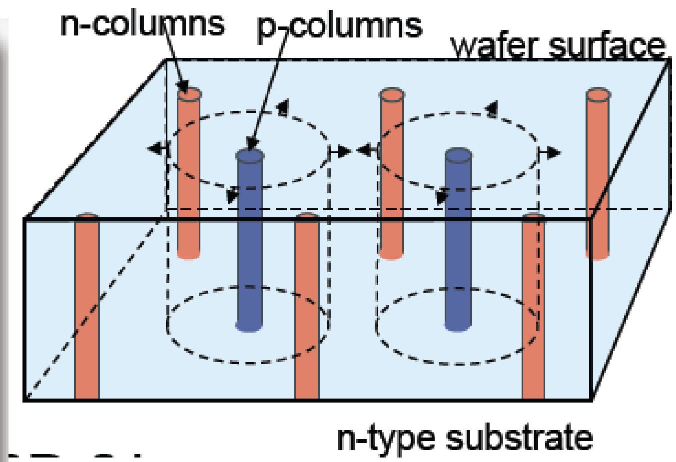

- Implants through the detector
- Highly segmented sensor
- Low depletion voltage
- Fast signal
- High rate capable
- Inefficiency regions correspinging to column
- Low cost large production to be proven

The ATLAS PPS Project

- Aim: Explore the suitability of planar pixel sensors for highest fluences
- Approved ATLAS R&D project since 2009: 17 institutes, more than 80 scientists

ATLAS project	R&D on Planar Pixel Sensor Technology for the ATLAS Inner Detector Upgrade		
ATLAS Upgrade Document No:	Institute Document No.	Created: 10/01/2008	Page 1 of 19
		Modified: 07/05/2009	Rev. No.: 1.1

D. Dobos, B. Di Girolamo, H.Pernegger, S. Roe, A. La Rosa[1], V. Vrba, P. Sicho, J. Popule, M.Tomasek, L. Tomasek, J. Stastny, M. Marcisovsky, M. Havranek, J. Bohm[2], A. Lounis, N. Dinu, M. Benoît, R. Tanaka[3], G. Calderini, D. Lacour, H. Lebbolo, G. Marchiori, J. Ocariz, P. Schwemling[4], M. Barbero, F. Hügging, H. Krüger, N. Wermes[5], H. Lacker[6], I. M. Gregor, U. Husemann, P. Kostka[7], C. Gößling, R. Klingenberg, D. Münstermann, A. Rummler, G. Troska, T. Wittig, R. Wunstorf[8], J. Grosse-Knetter, M. George, A. Quadt, J. Weingarten[9], L. Andricek , M. Beimforde, A. Macchiolo, H.-G. Moser, R. Nisius, R. Richter, P. Weigell[10], D. Cauz, M. Cobal, C. del Papa, D. Esseni, M. P. Giordani, P. Palestri, G. Pauletta, L. Selmi[11], Y. Unno, S. Terada, Y. Ikegami[12], M. Cavalli, I. Korolkov, M. Lozano, C. Padilla, G. Pellegrini, M. Ullan[13], T. Affolder, P. Allport, G. Casse, T. Greenshaw, I. Tsurin[14], M. Battaglia, T. Kim, S. Zalusky[15], I. Gorelov, M. Hoeferkamp, S. Seidel, K. Toms[16], V. Fadeyev, A. Grillo, J. Nielsen, H. Sadrozinski, B. Schumm, A. Seiden[17]

17 institutions: [1]CERN, [2]AS CR, Prague, [3]LAL Orsay/ University Paris-sud XI, [4]LPNHE / University Paris VI, [5]University of Bonn, [6]HU Berlin, [7]DESY, [8]TU Dortmund, [9]University of Goettingen, [10]MPP and HLL Munich, [11]Università degli Studi di Udine – INFN, [12]KEK, [13]IFAE-CNM (Barcelona), [14]University of Liverpool, [15]UC Berkeley/LBNL, [16]UNM, Albuquerque, [17]UCSC, Santa Cruz

Why planar sensors?

- Planar pixel is a proven technology
  - The current n-in-n pixel detector.
  - Modules shown to work after $10^{15}\ n_{eq}/cm^2$
  - If strips not adequate any more, pps would be the natural option

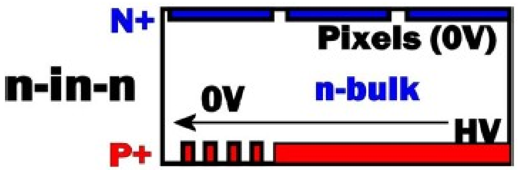

- Potential for a low-cost large-area production with n-in-p
  - Only one side is patterned

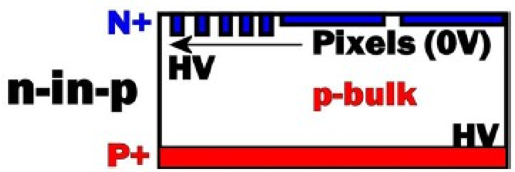

- Research directions
  - Advanced simulation studies
  - Active area optimization and geometry redesign
  - Radiation damage studies
  - High rate capable electronics
  - Low cost module production

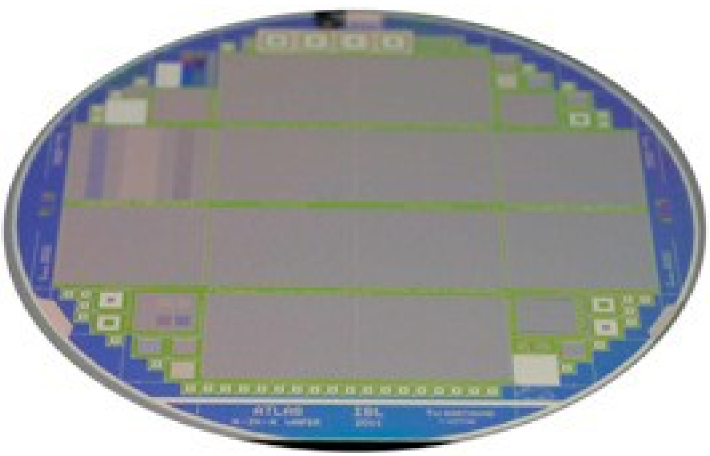

PPS working "tools"

- Different sensors, n- & p-type bulk both FEI3 and FEI4

CiS

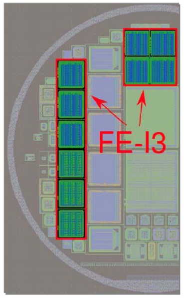

Micron

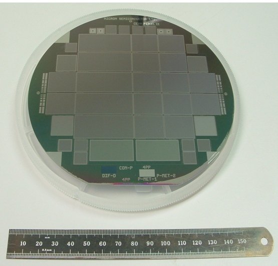

HPK

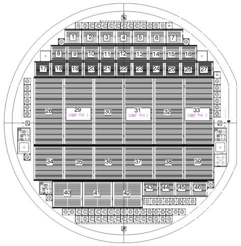

MPI-HLL

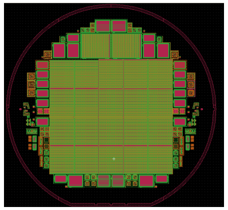

- n&p irradiation up to $2x10^{16} n_{eq}/cm^2$

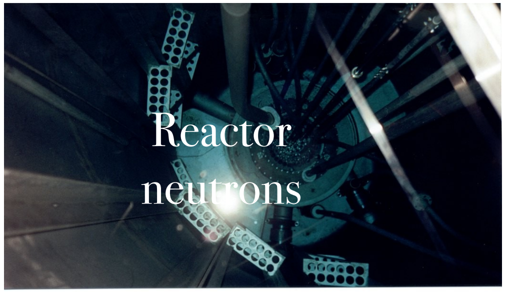

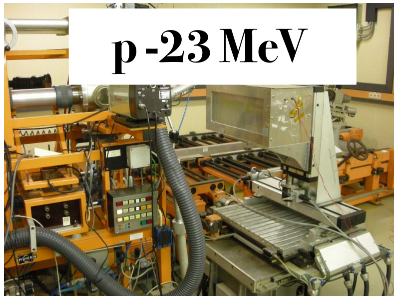

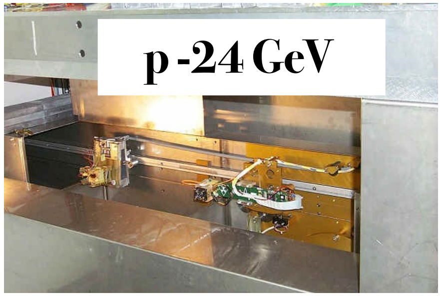

- Lab characterization & beam tests

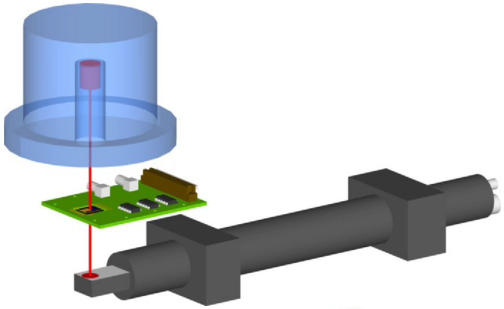

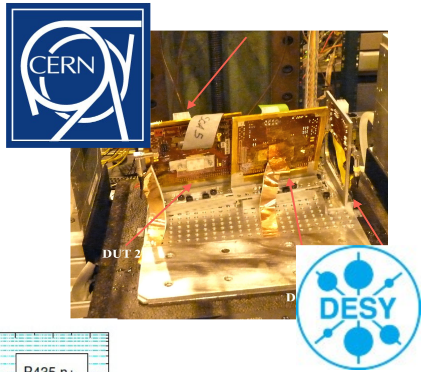

- TCAD simulations along with precise inputs

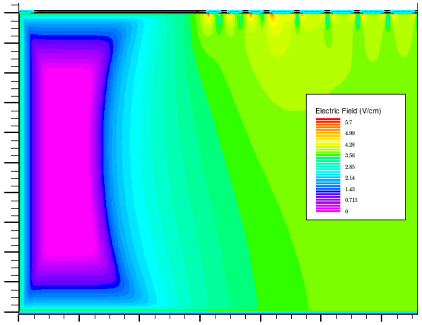

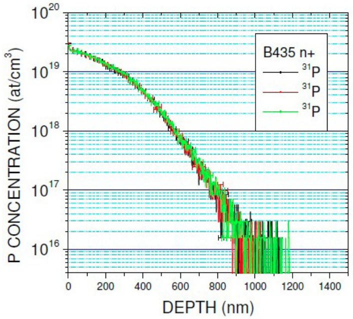

TCAD Simulations

- Technology Computer Aided Design offers the possibility to simulate the behavior of a sensor under several conditions
  - Reverse bias
  - Illuminated by light
  - At high/low temperature
  - As been exposed to high fluences

Simulation saves you money but needs very precise inputs to produce reliable information

- And monitor the interesting quantities
  - IV / CV curves
  - GR potentials
  - CCE
  - Electric field

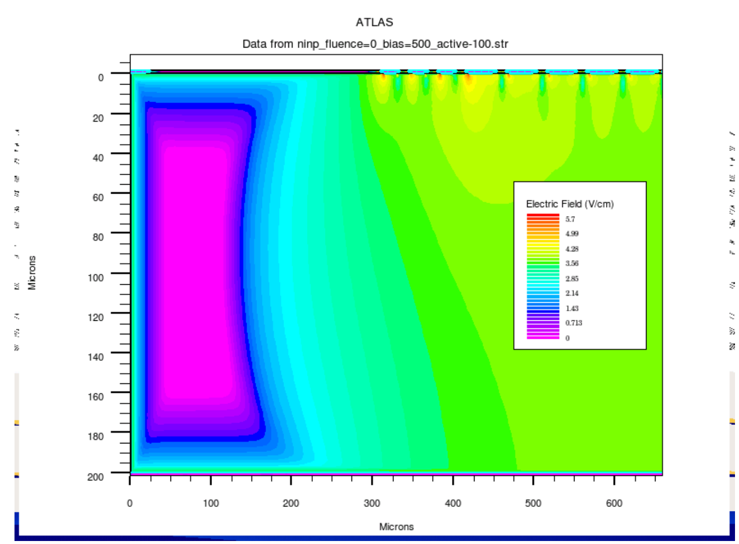

Sensor tested in lab & on beam

- Sensors bonded to FEI3 or FEI4 ROCs are tested in the laboratory with the help of radioactive sources and in a beam test setup equipped with a beam telescope which allows tracking

Single chip adapter card w/ sensor + FE

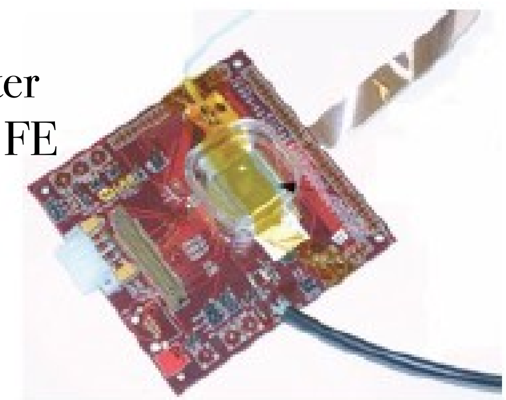

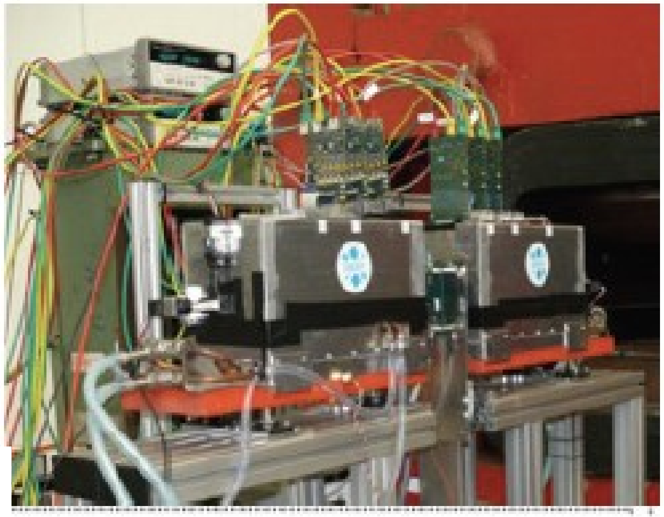

Test beam:
- hit maps
- energy deposition
- efficiencies
- spatial resolution

Source scans:
hit maps &
energy deposition

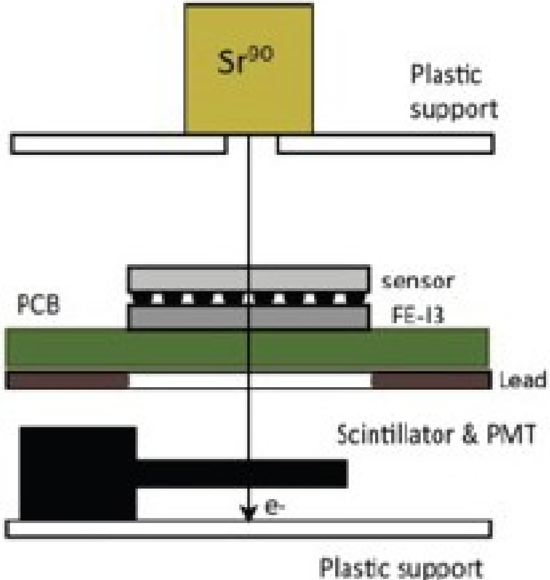

One or several DUTs

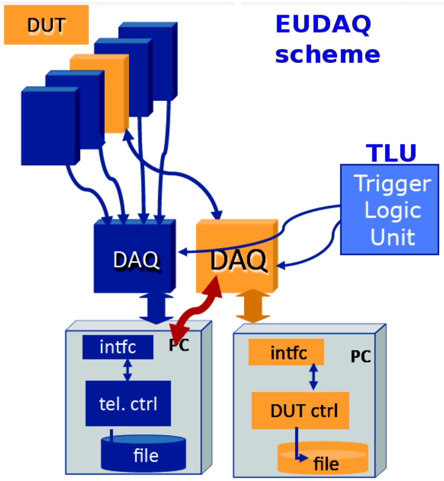

Cooling system

N-in-n Charge collection

- **Status** ATLAS pixels modules were shown to be rad-hard up to 10^{15} n_{eq}/cm^2
  - **Goal**: test further their radiation tolerance, up to $2x10^{16}$ n_{eq}/cm^2

→**Method**: n-irradiated (Φ up to $2x10^{16}$ n_{eq}/cm^2) ATLAS modules tested with β from source and π/e beams

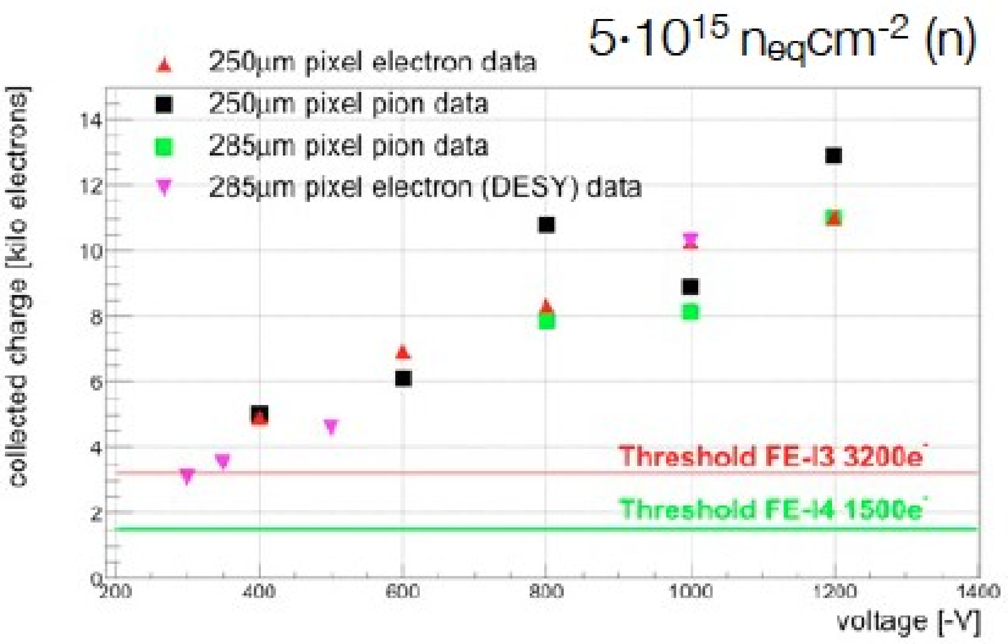

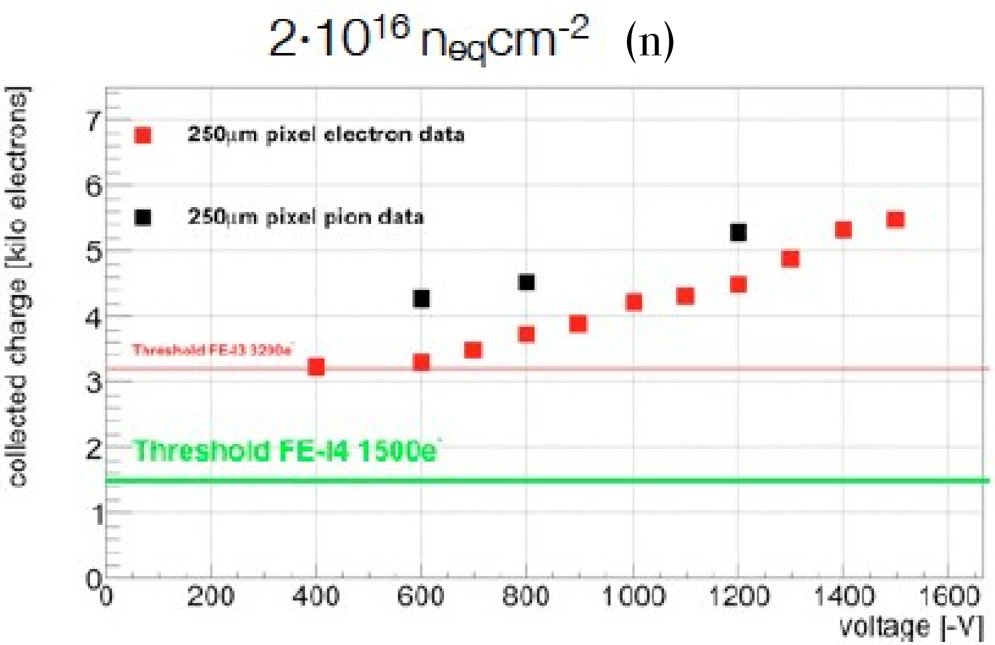

→**Result**: Charges are higher than model predictions which include trapping

Intermezzo: charge multiplication

→ 140 and 300 μm n-in-p Micron sensors after $5x10^{15}$ n_{eq} 26MeV protons

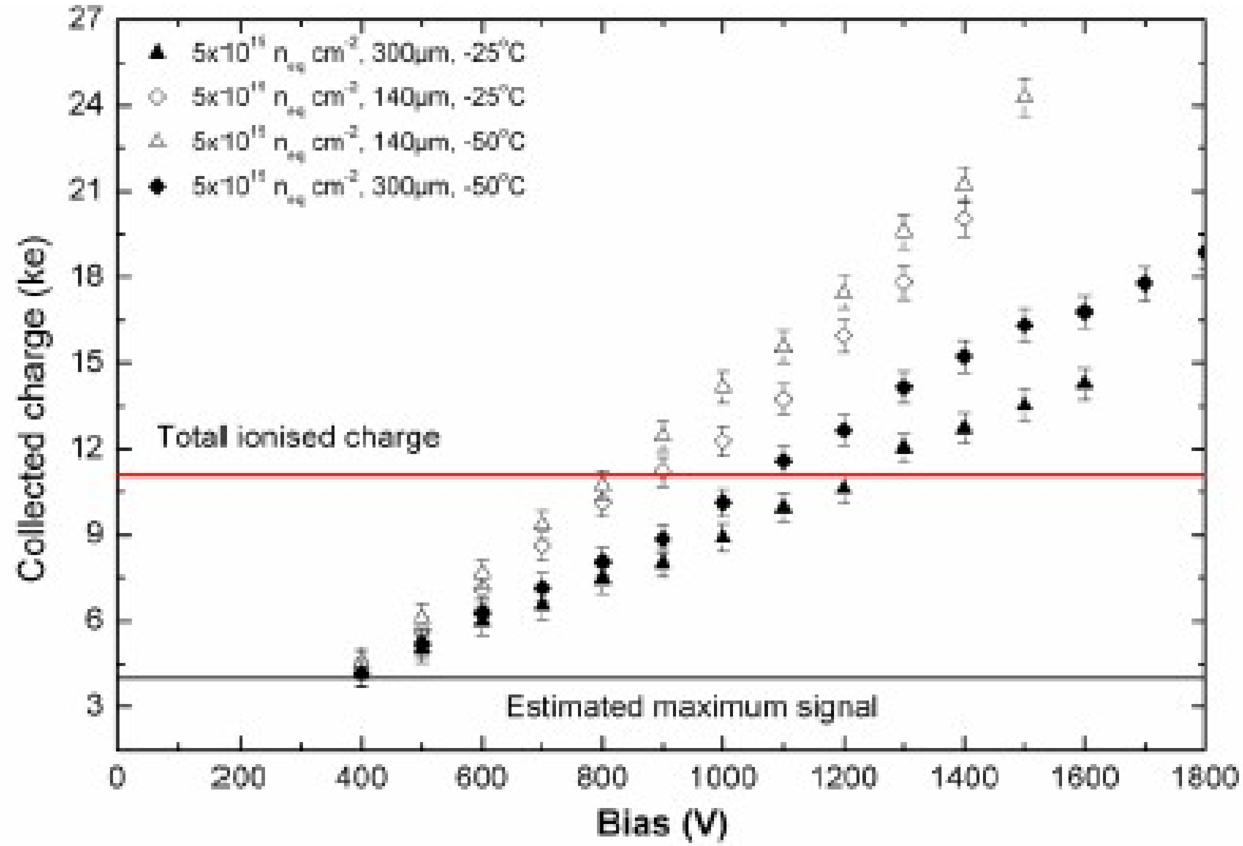

✔ Evidence of a charge multiplication effect: not only the whole charge is recovered, but increased by f = 1.75

N-in-n hit efficiency

- **Status**: after irradiation the full depletion voltage changes → bulk could be only partially depleted
- **Goal**: fully recover the hit efficiency
- **Method**: increase bias voltage for n-&p-irradiated modules

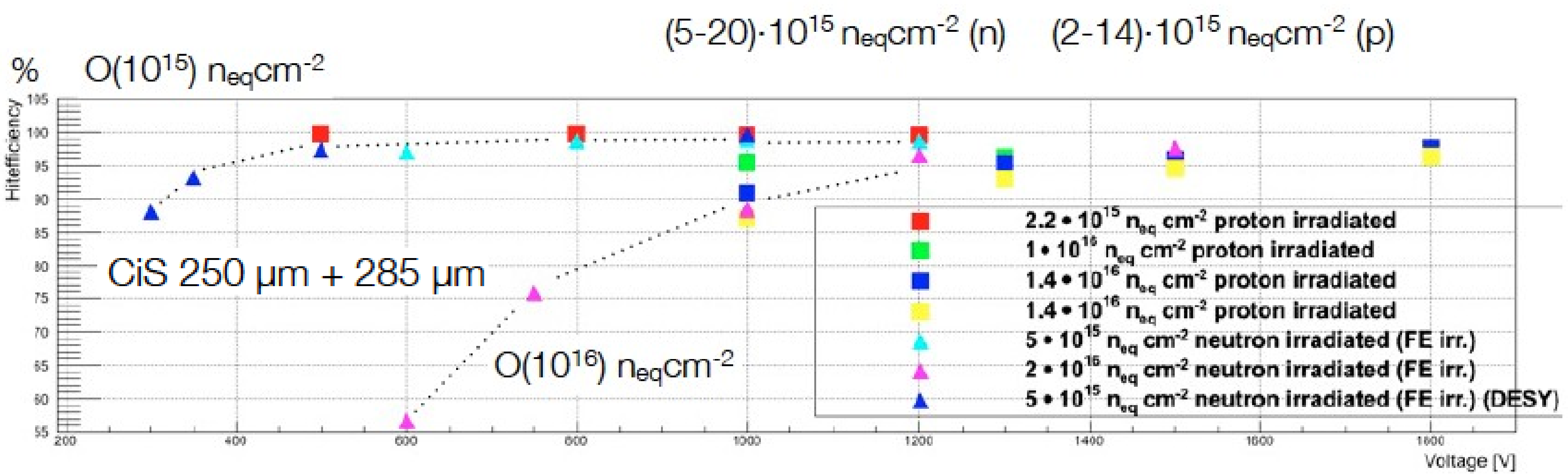

- **Result**: efficiency recovered at V_{bias}=1000V for fluences up to $5x10^{15} n_{eq}/cm^2$ and very promising results for $\Phi \sim O(10^{16} n_{eq}/cm^2)$

N-in-n "in-pixel" efficiency

- **Goal**: identify in-efficient regions inside the pixel cell
- **Method**: test on beam irradiated device ($4x10^{15}n_{eq}/cm^2$ (n), 250 μm), studying their efficiency as a function of the V_{bias}
- **Result**: <ε> > 97% @ 600V

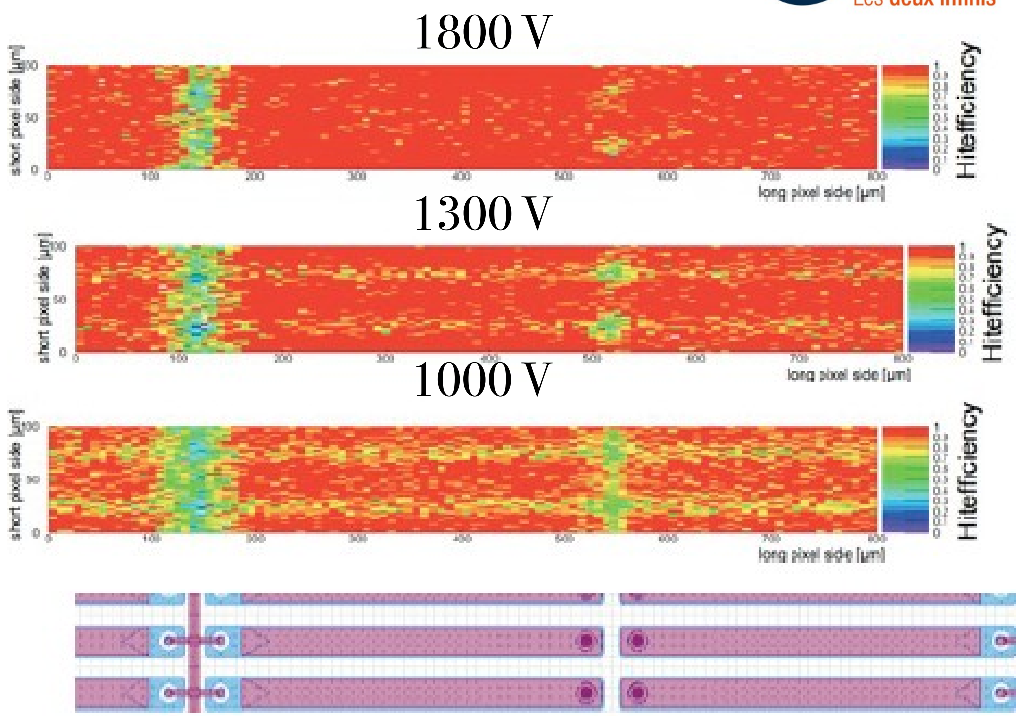

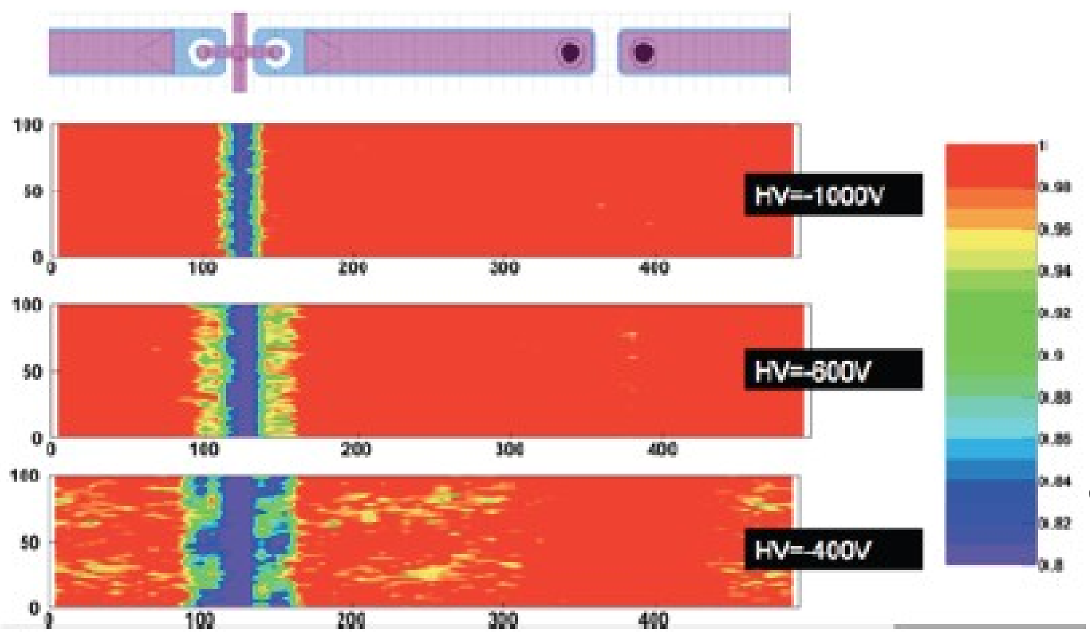

- **Method**: test on beam irradiated device ($1.4x10^{16}n_{eq}/cm^2$ (p), 250 μm), studying their efficiency as a function of the V_{bias}
- **Result**: <ε> > 97% @ 1800V

N-in-p charge collection

- **Goal**: test charge collection for p-bulk detectors at $\Phi \sim O(10^{15} n_{eq}/cm^2)$
- **Method**: 285 μm thick n-in-p sensors, n-irradiated, tested with radioactive source

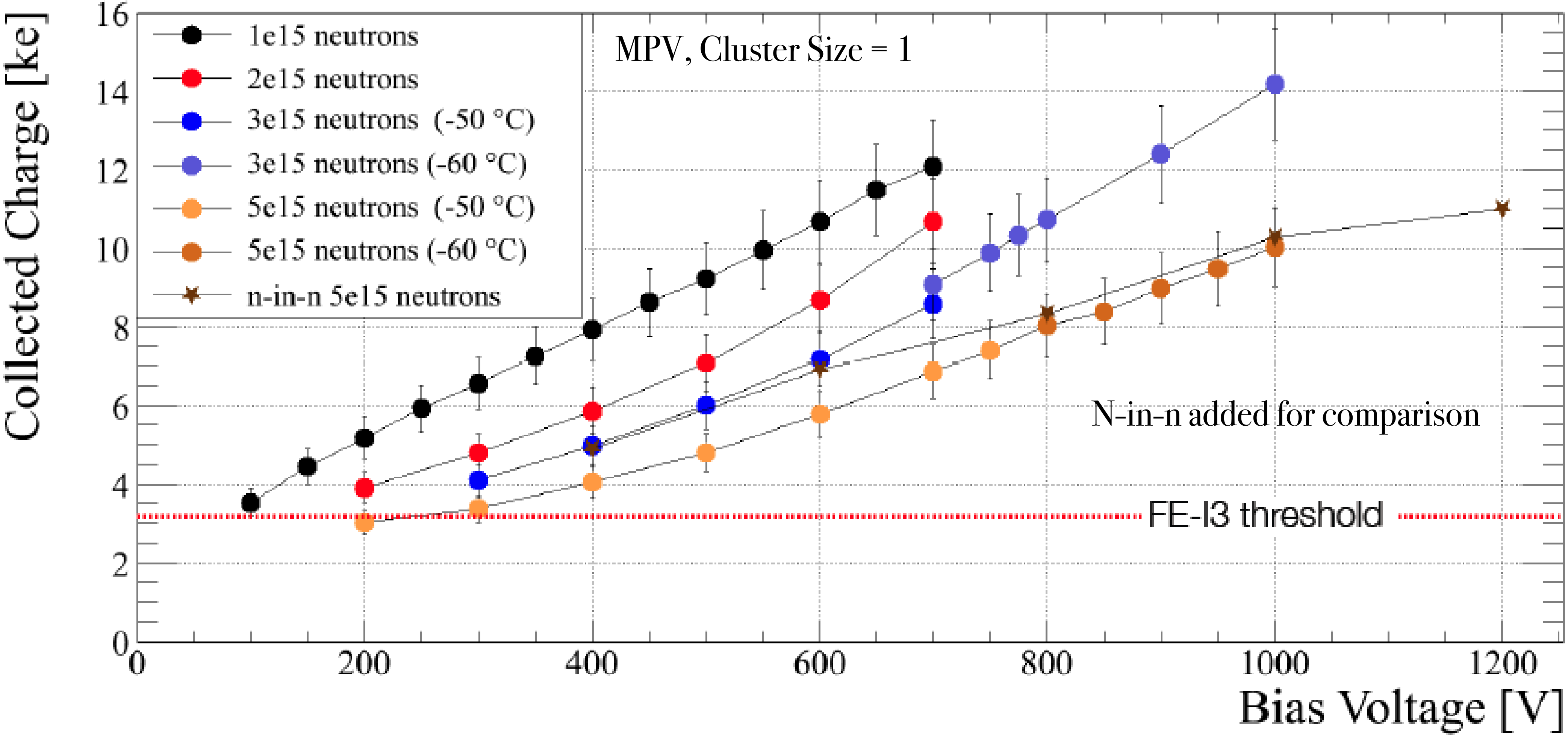

- **Result**: significant charge is collected above threshold, V_{bias} > 600 V

N-in-p "in-pixel" efficiency

- **Goal:** identify in-efficient regions inside the pixel cell

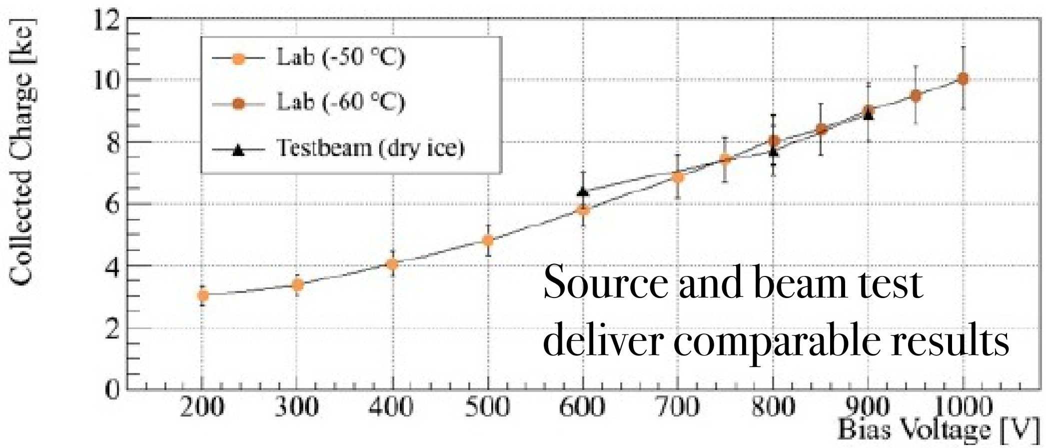

- **Method**: 300 µm thick, neutron-irradiated @ $5x10^{15} n_{eq}/cm^2$

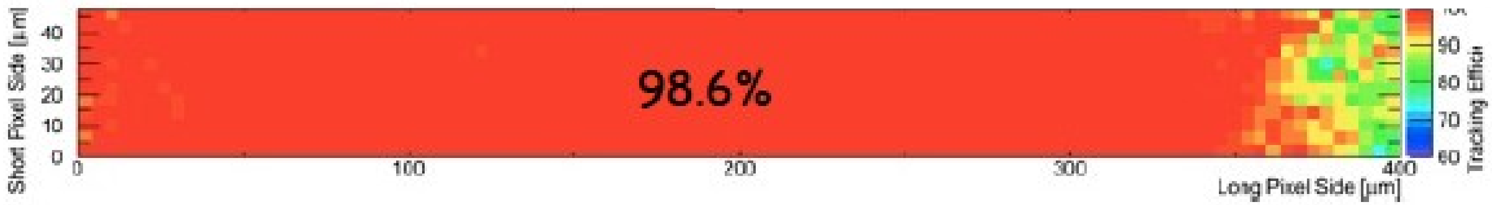

- **Results:**
  - significant charge is collected above threshold
  - overall efficiency :98.6%;
  - losses around bias dot; higher efficiency in the center of the pixel

Thin bulk sensor

- **NEW**: first HPK n-in-p sensors, 150 μm, 6" wafer with different pixel biasing and isolation schemes

→ Bias structure aims to reduce less-efficient area

A) Punch-thru (PTLA): a bias dot in the 4-corner

B) Polysilicon: an encircling pixel implant (~2MΩ)

→ Isolation structure:

I. P-stop, common & individual

II. p-spray

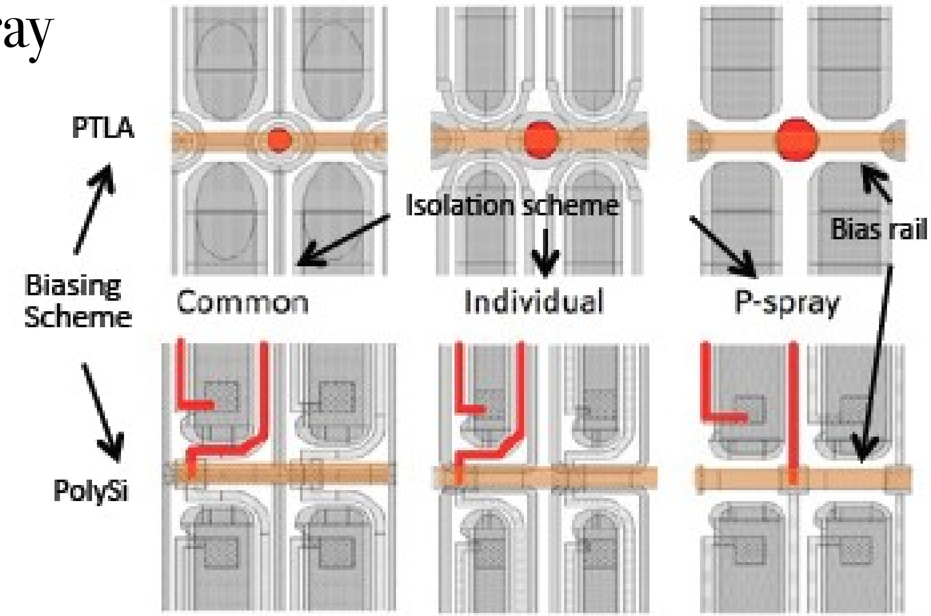

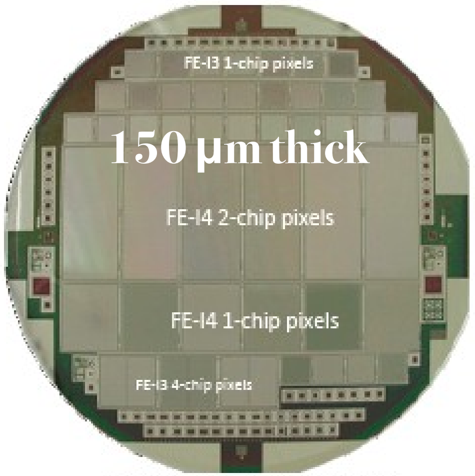

HPK n-in-p 6-in. wafer

Investigated on beam. See next slides

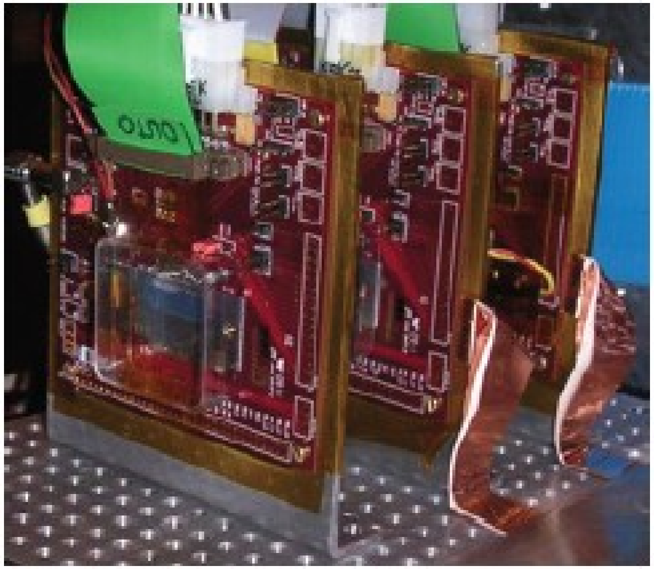

Thin bulk sensors on beam

- non-irrad: FDV ~ 40 V, saturated > 40 V operated at 150 V bias voltage in test beam
- shown are "in-pixel" efficiency of non-irradiated FE-I4 samples
- p-stop common on Poly Silicon shows best

efficiency map

- slight inefficiency beneath the bias rail

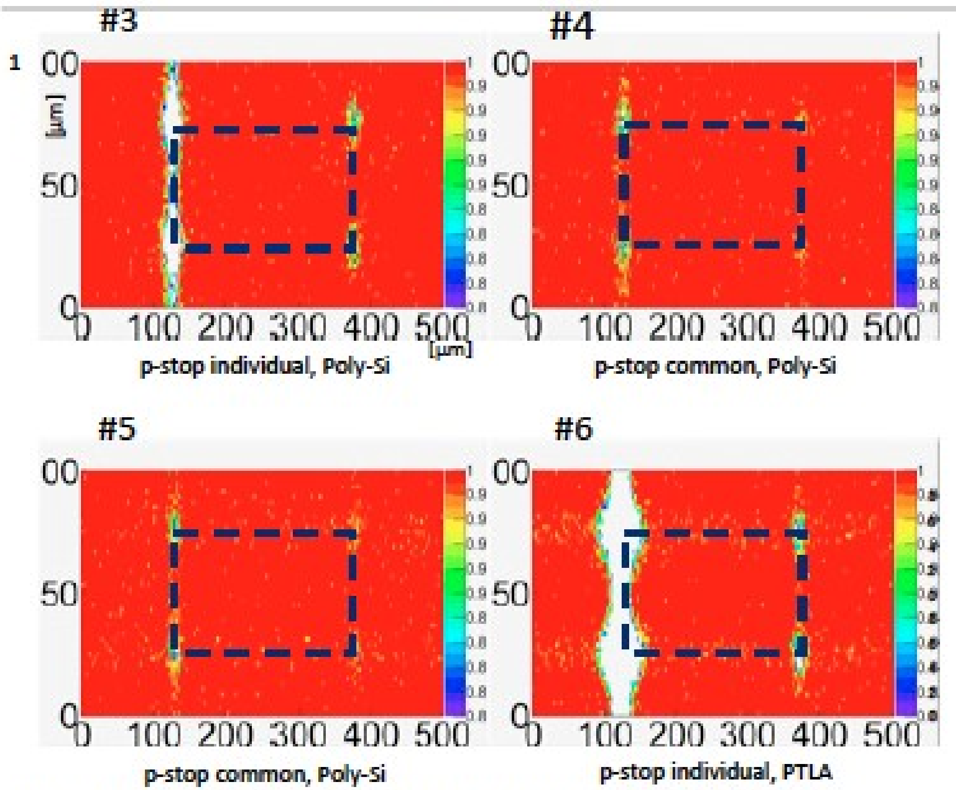

2D efficiency map of a pixel, non-irrad, at 150 V bias voltage

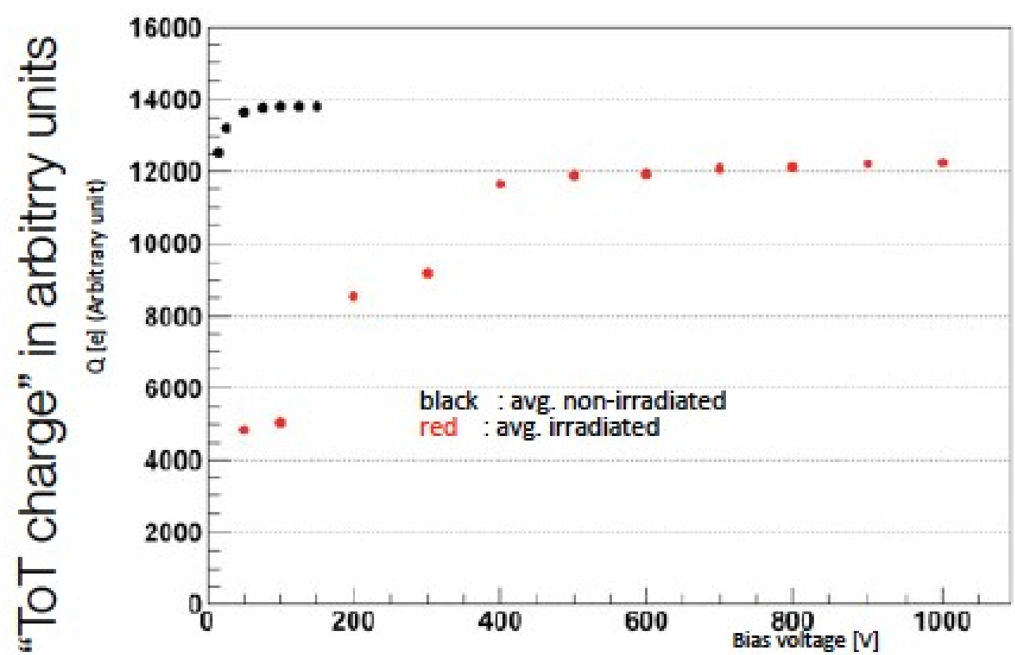

Bias voltage dependence of collected charges

Note: independent charge calibration for non-irradiated and irradiated samples.

- 4 FE-I4 samples also investigated after irradiation $2{\cdot}10^{15}\,n_{eq}\,cm^2$ (FE-I4)
- 2x PolySi-common p-stop: KEK4,5
  PolySi-individual p-stop: KEK3
  PTLA-individual p-stop: KEK6

Geometry – Dead edge

Dead edge is an inactive area whose purpose is to protect the cut area (full of generation centers) from high electric field

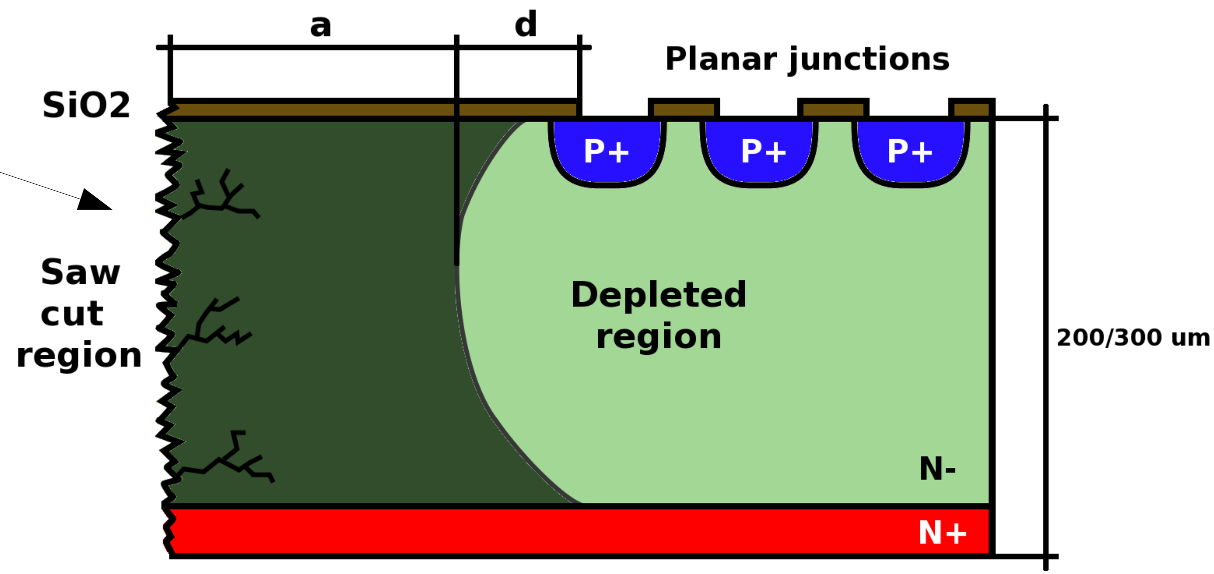

- "It is not possible to obtain the full geometrical coverage in z as the Pixel detector does, where modules are tilted in z and are partially overlapped, because there is not enough space. However the gap between modules is minimized using a sensor design with active or slim edges." IBL TDR

Geometry optimizations

SLIM EDGES

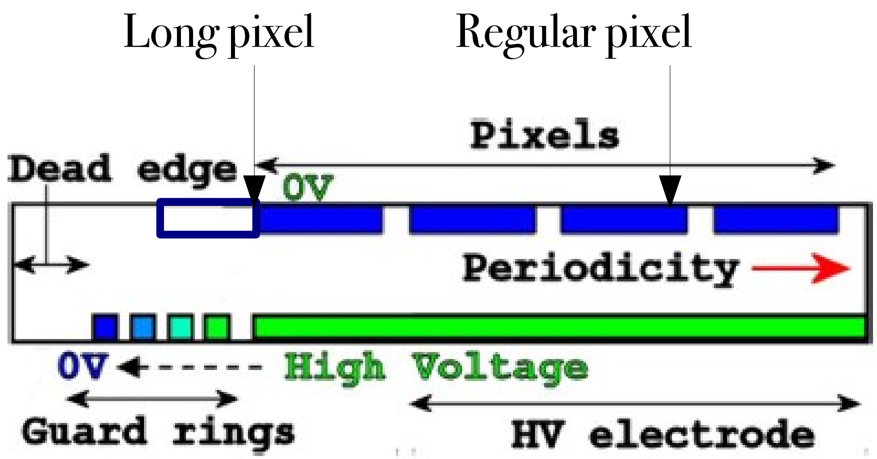

n-in-n

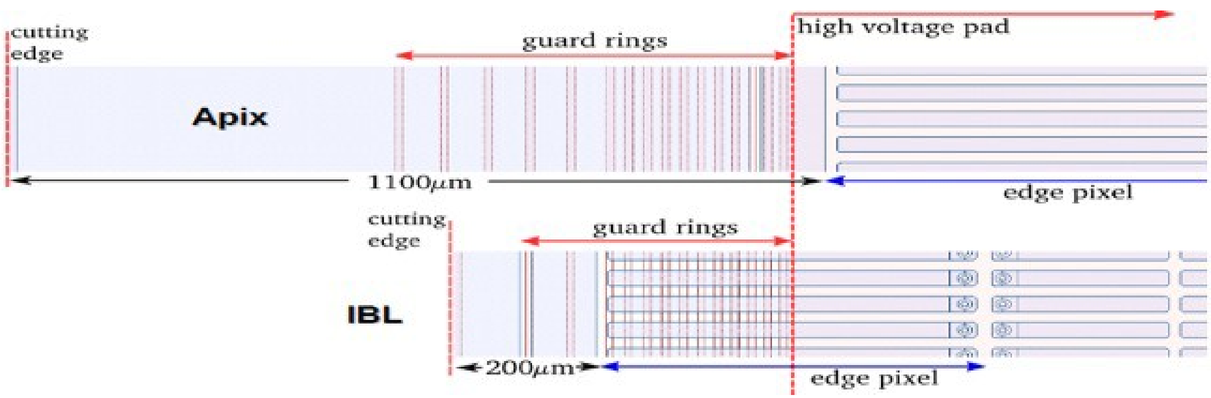

Longer pixel “under the guard-ring”

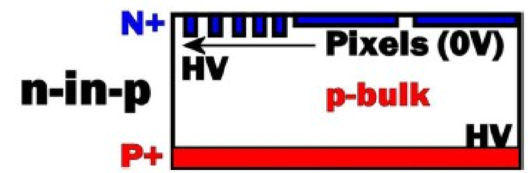

n-in-p

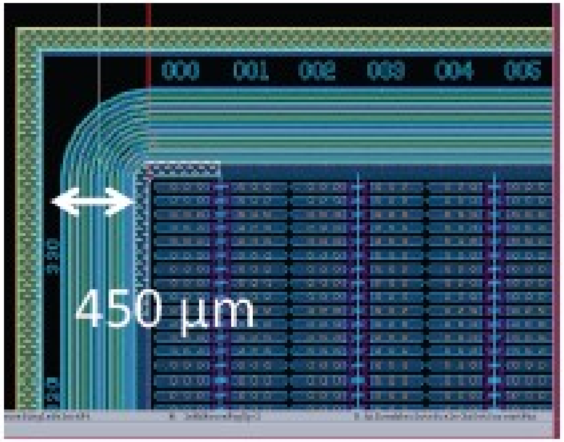

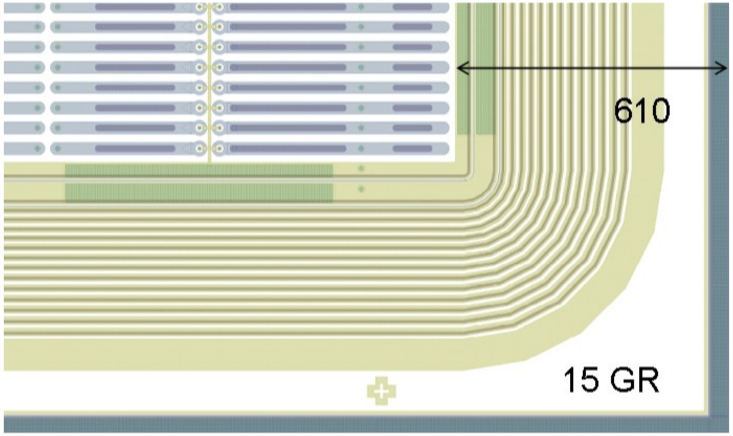

Intermezzo: simulations

Design: "stepwise pixels"

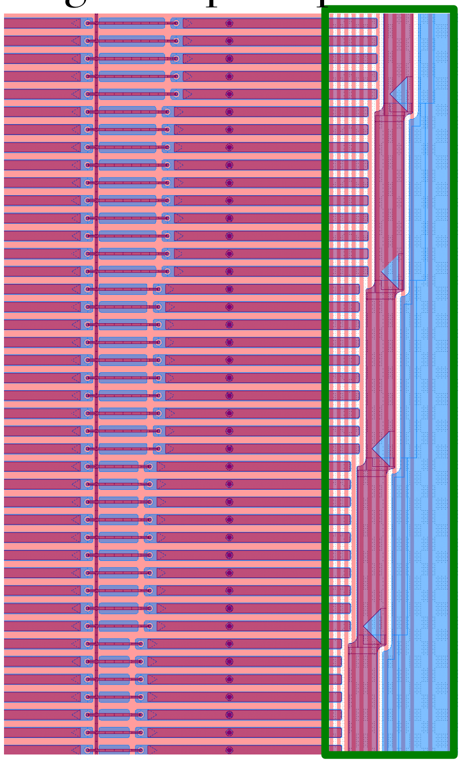

SIMS measurements: determining doping profiles

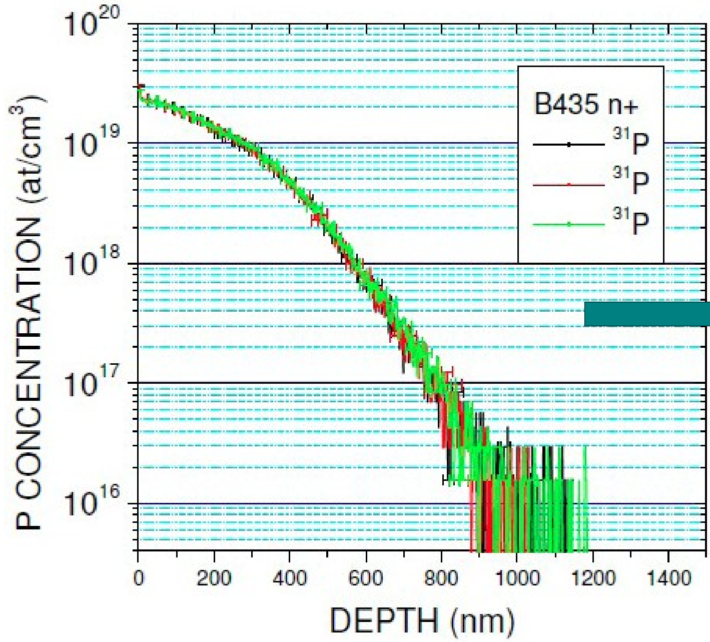

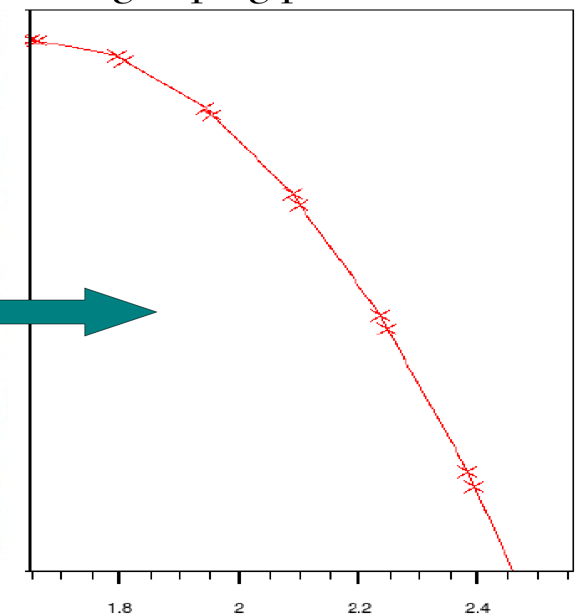

Potential before irradiation for a slim edge structure

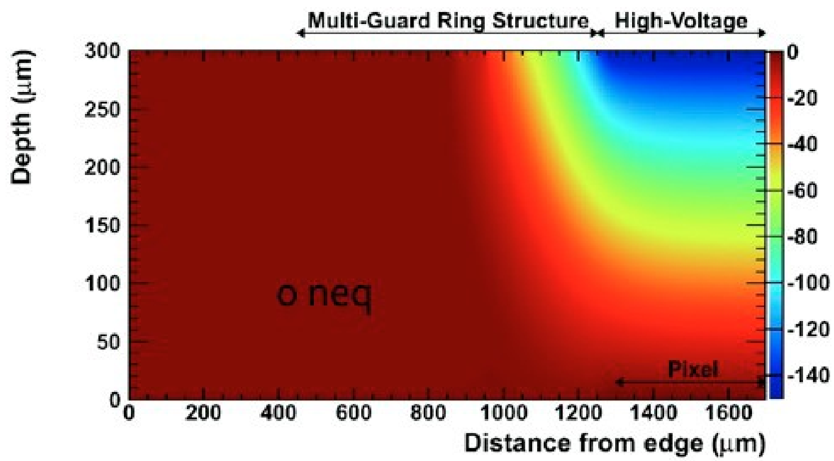

Potential after irradiation for a slim edge structure

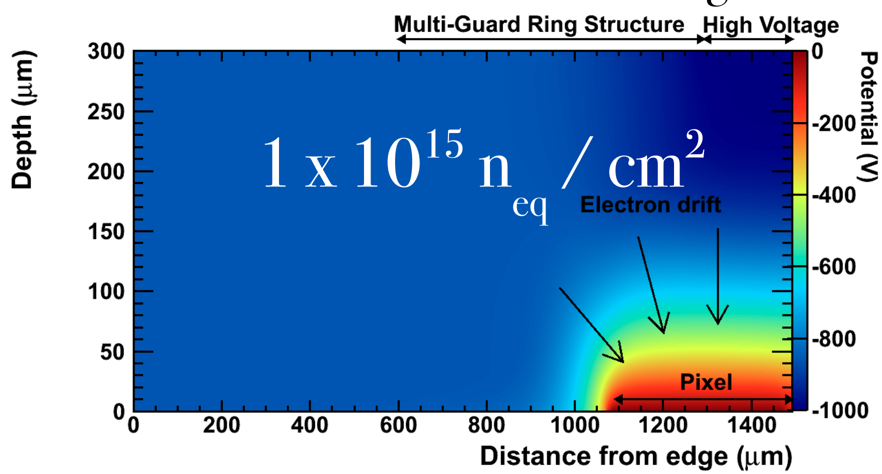

SIMS measurements

- SIMS: Secondary Ion Mass Spectroscopy

Cameca SC-Ultra

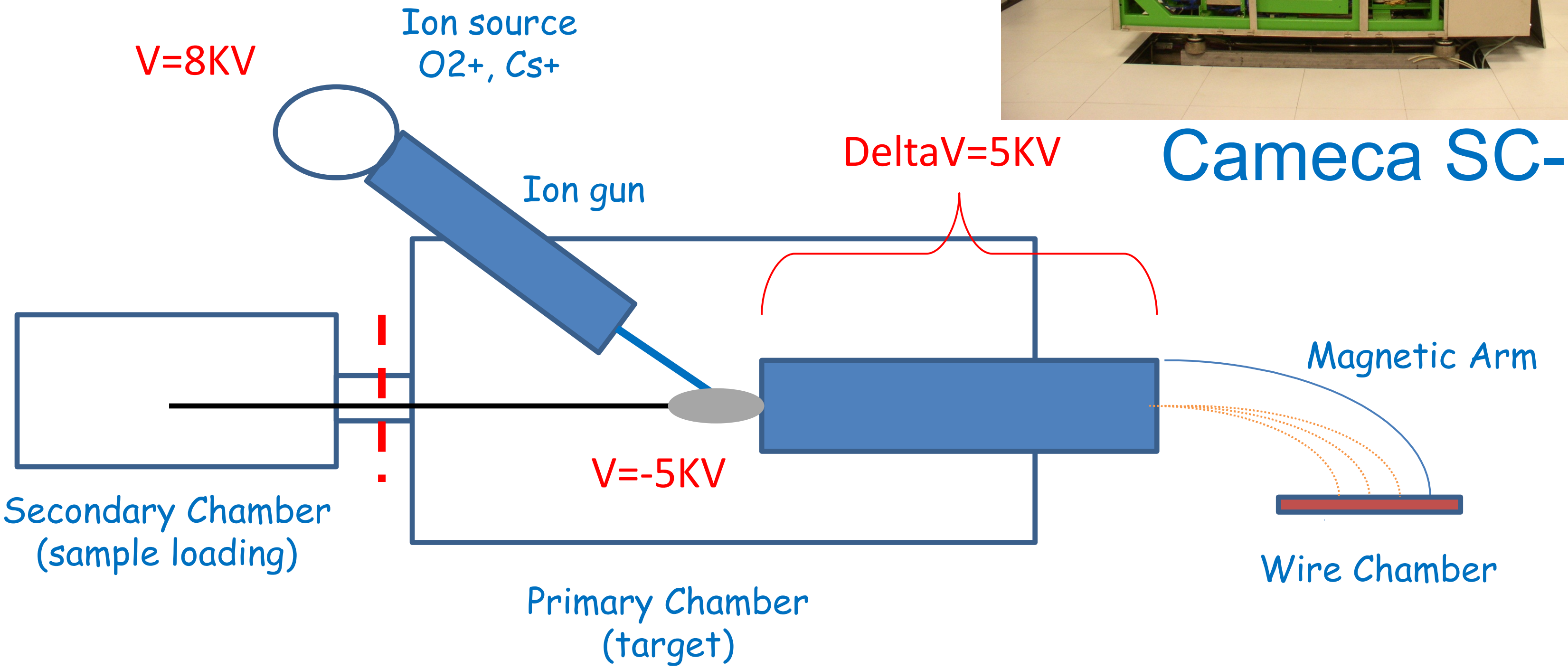

SIMS principle

- An ion beam is scanning (and escavating the sample)

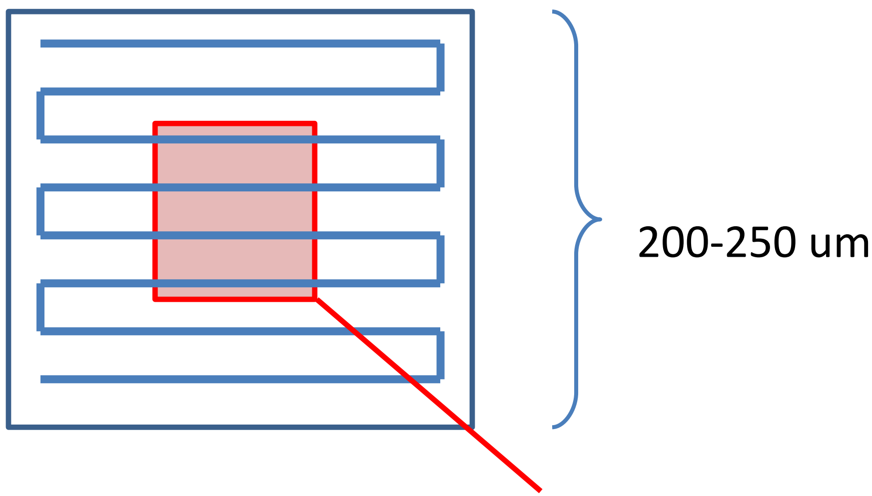

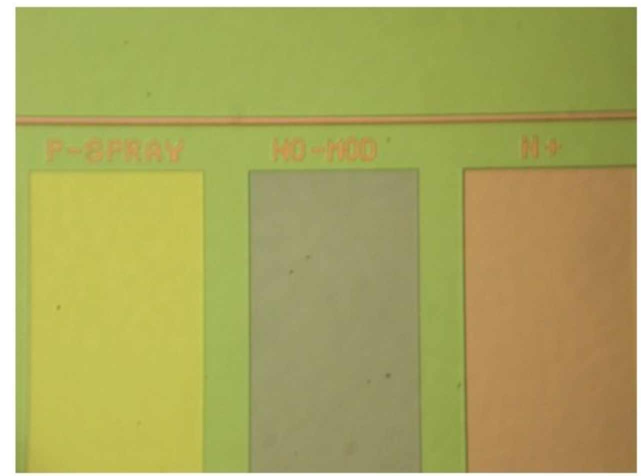

Restricted region analyzed
(to avoid scattering from walls)

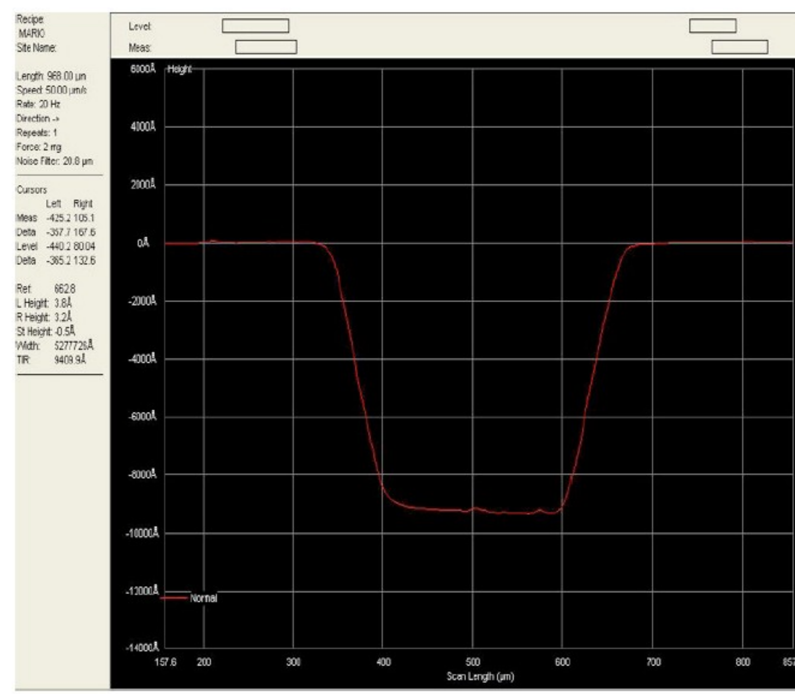

Measured with AFM

Intermezzo: test beams

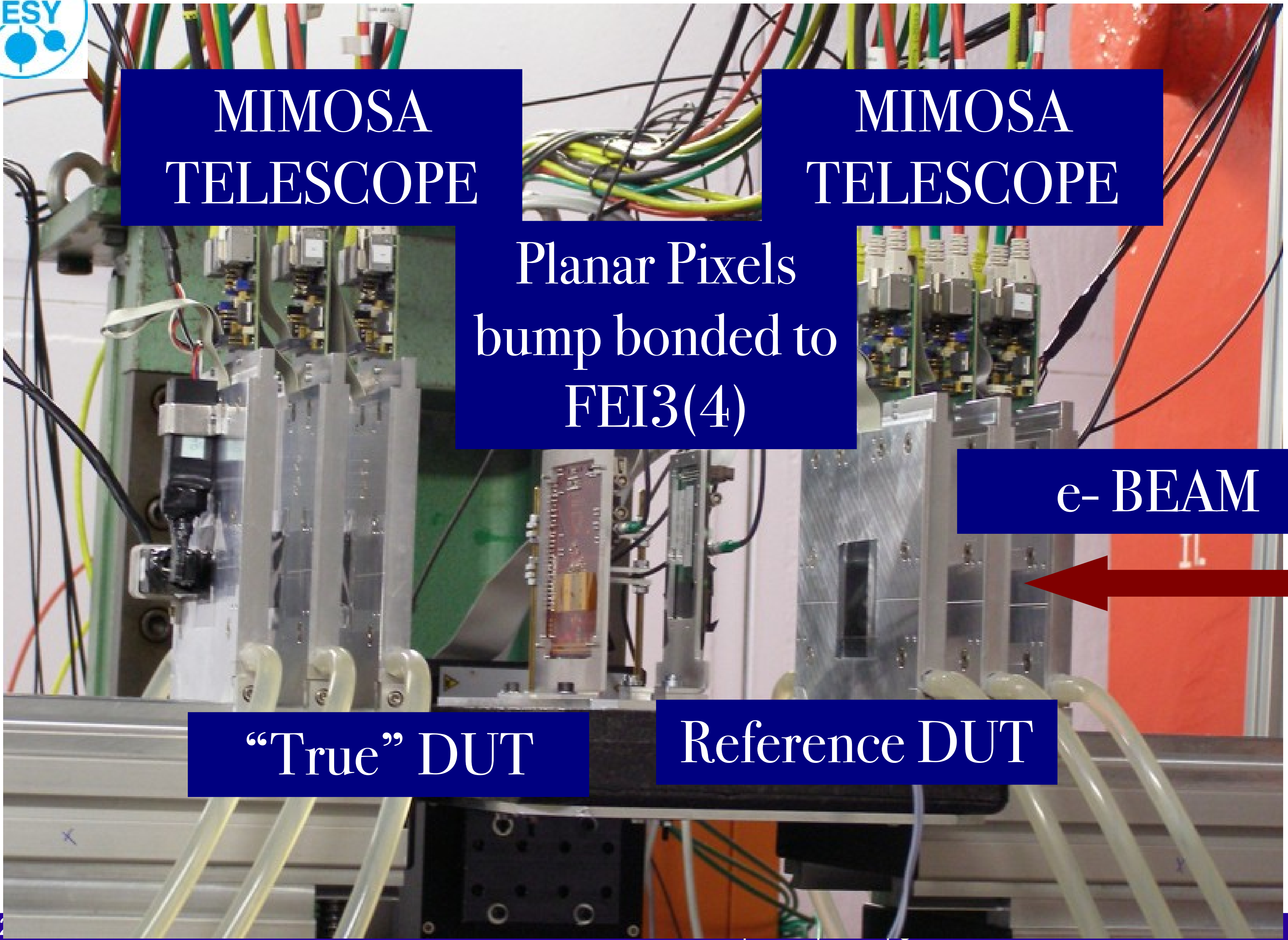

Beam test configurations

September: CERN SPS (H6B), high-eta DUT setup

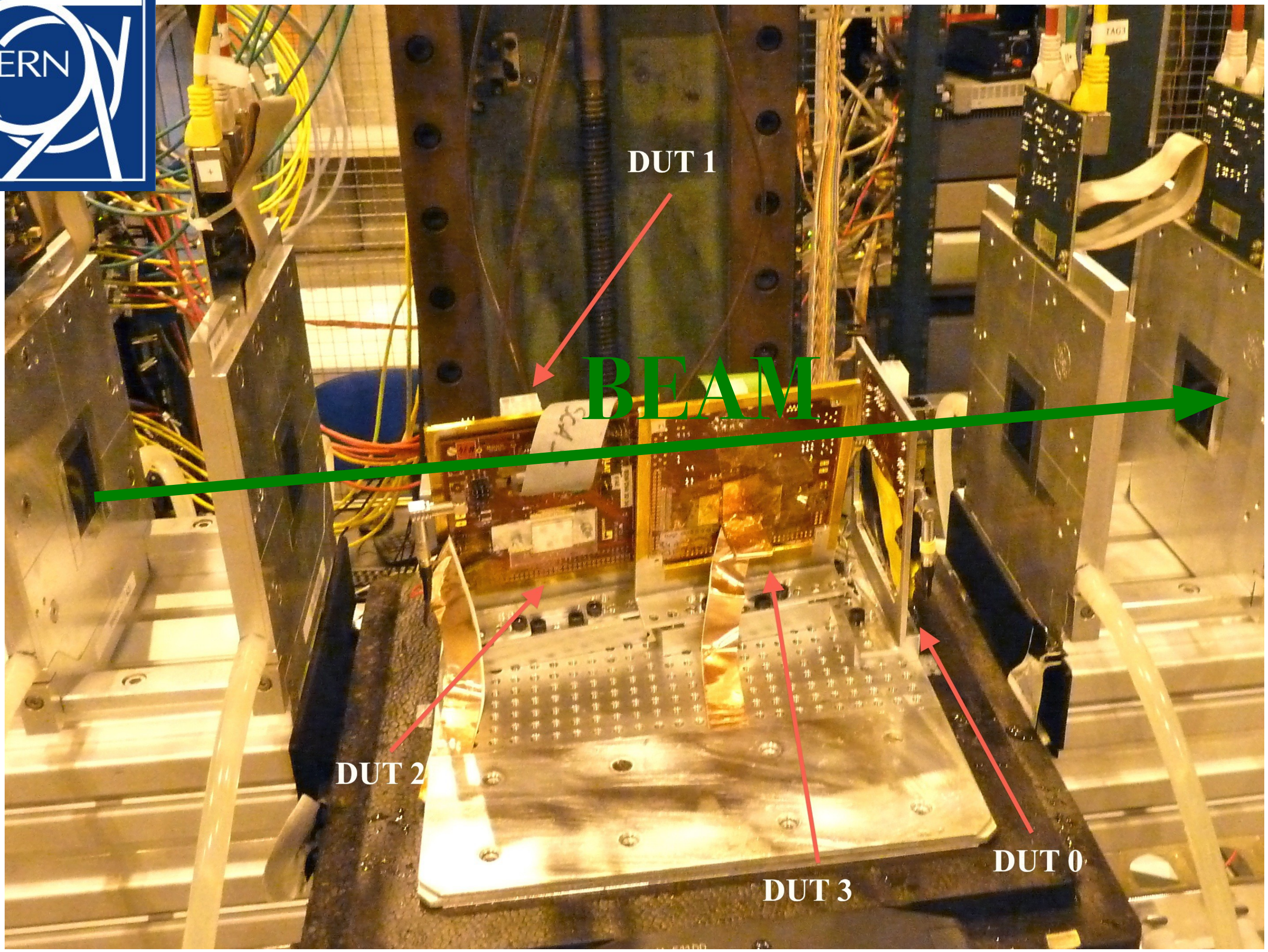

Performance of the telescope

Pointing resolution in between the planes

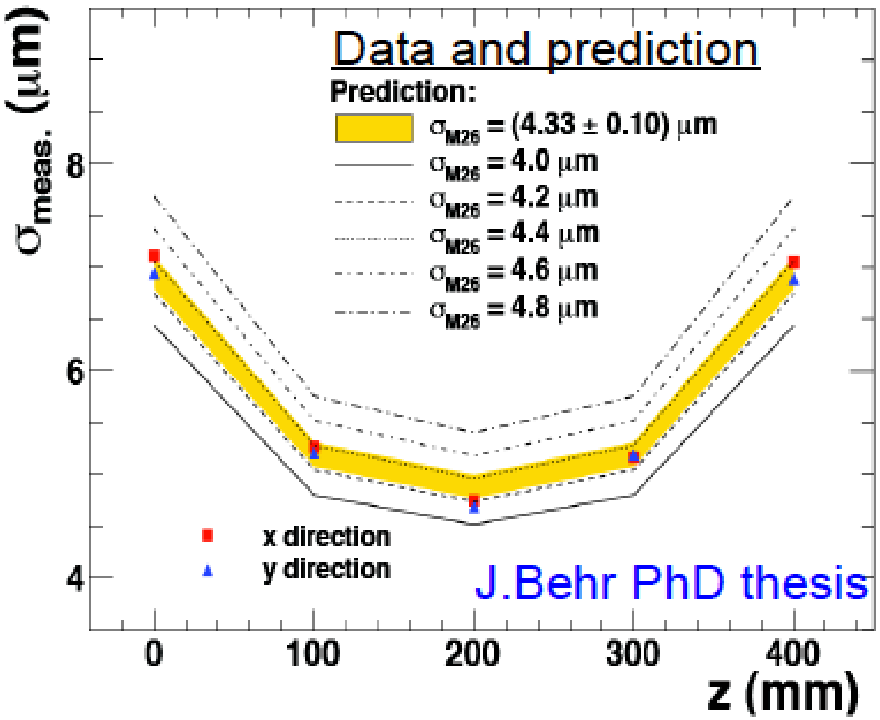

$$\sigma^2_{meas} = \sigma^2_{m26} + \sigma^2_{pointing\text{-}resolution}$$

Track extrapolation accuracy far behind the telescope planes

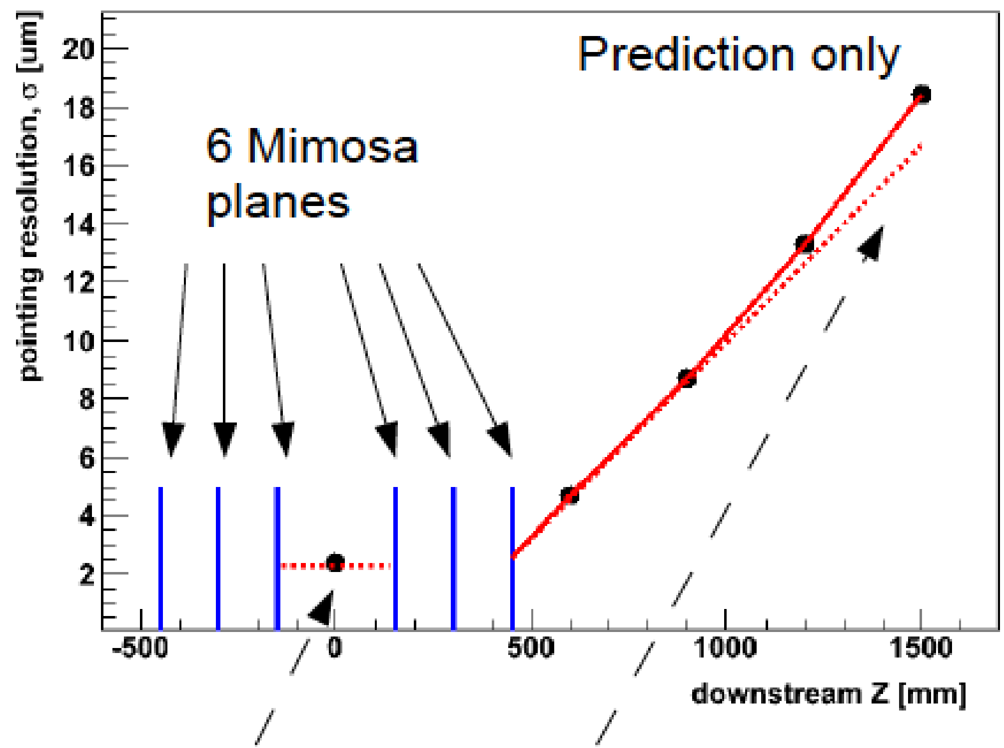

A DUT within the telescope arms
$\sigma \sim 2\ \mu m$

A DUT behind the telescope still can get a very reasonable track pointing resolution
$\sigma < 20\ \mu m$

Slim edge

- **Goal**: minimize inactive area, avoids shingling along beam axis
- **Method**: CiS n+-in-n with slim edges, 250 µm thick irradiated to $4 \cdot 10^{15}\,n_{eq}cm^{-2}$, data from pion test beam @ CERN
- **Result**: significant part of edge pixel sensitive
  - depends on HV and thickness, inactive edge reduced down to ~ 200 µm
- design chosen for the planar IBL sensor

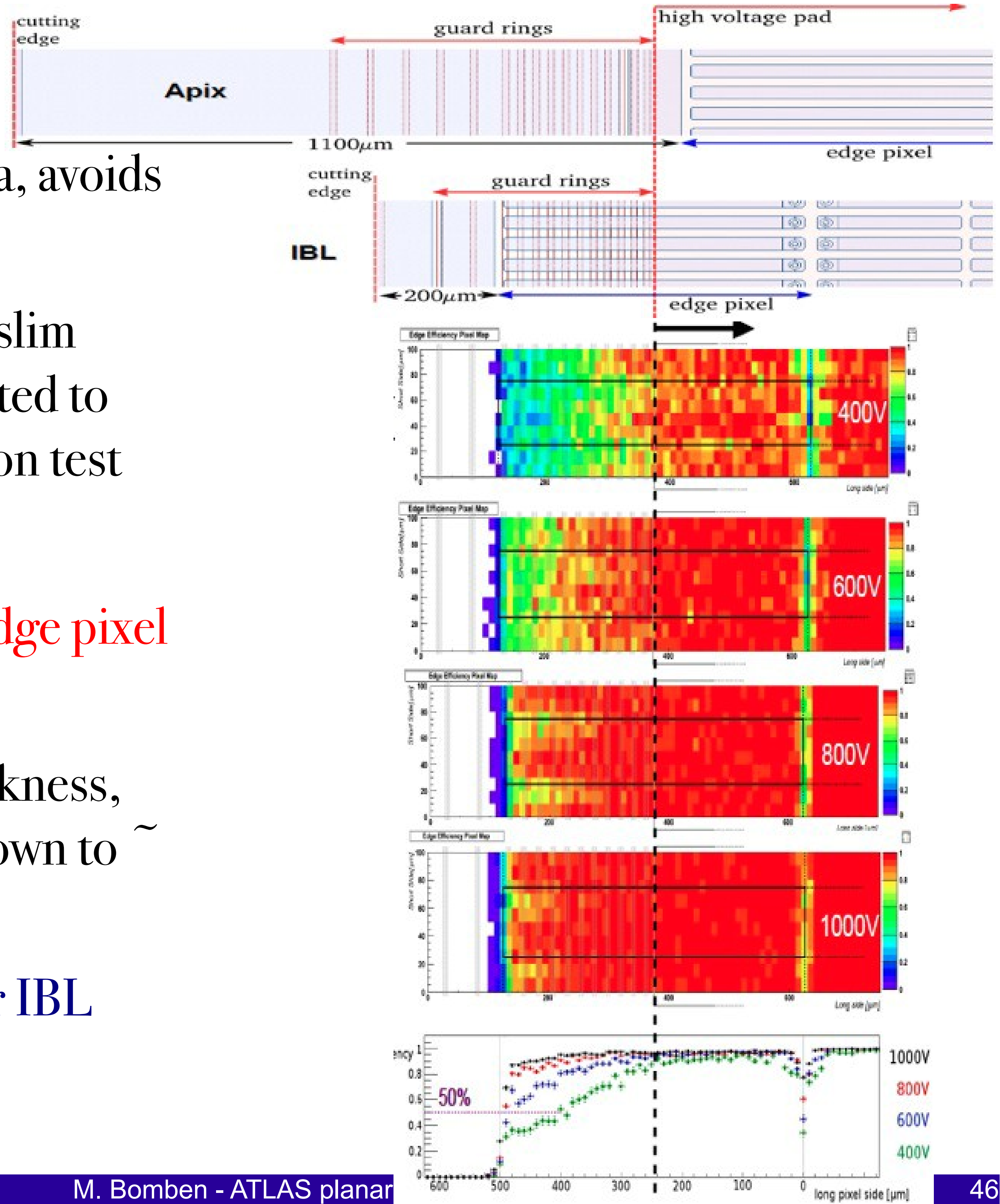

Active edge

- Another approach to reduce dead area
- Several ways to do that

➔ Drie-etching approaches
  - ✓ CNM/IFAE
  - ✓ FBK/LPNHE
  - ✓ VTT/Munich
  - ➢ <u>Easy to get thin wafers</u> → <u>inner layers?</u>

➔ Scribe + cleave + edge – passivation
  - ✓ UCSC
  - ✓ Dortmund
  - <u>Post-processing</u> →<u>outer layers?</u>

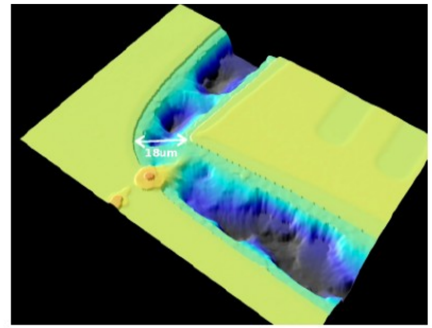

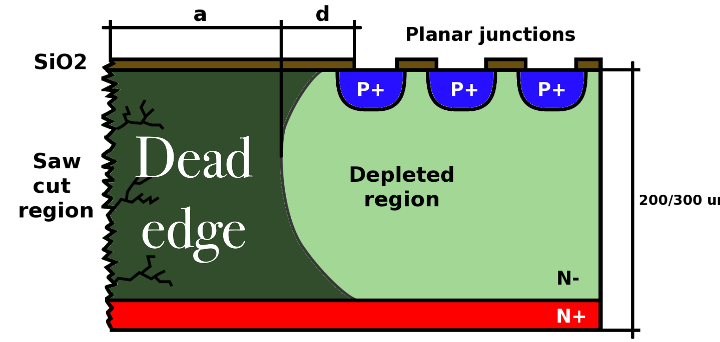

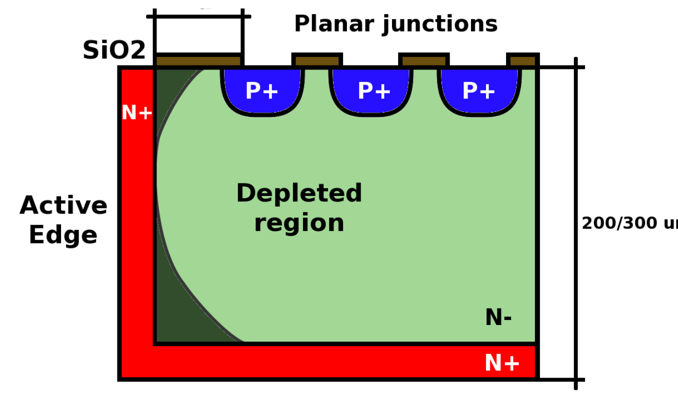

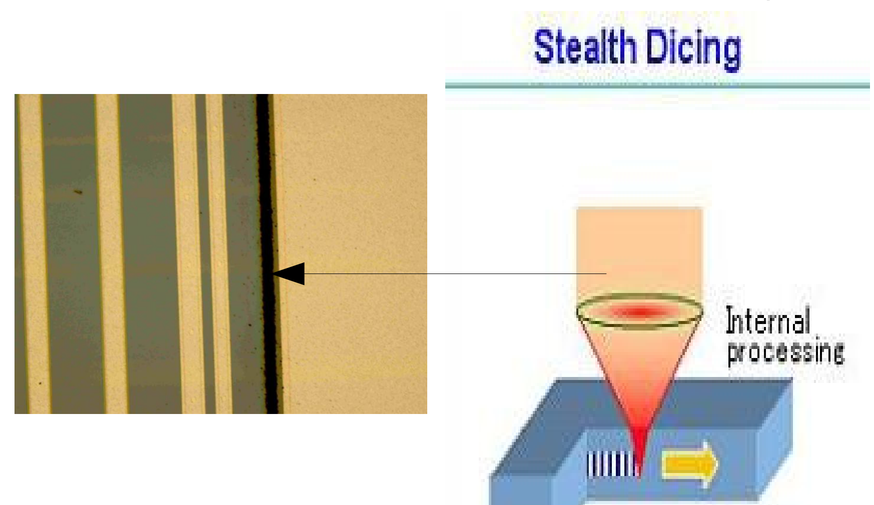

LPNHE – FBK active edge

M. Boscardin, A. Baglioni, G. Giacomini , N. Zorzi, E. Vianello, C. Piemonte, M. Povoli, G.F. Dalla Betta

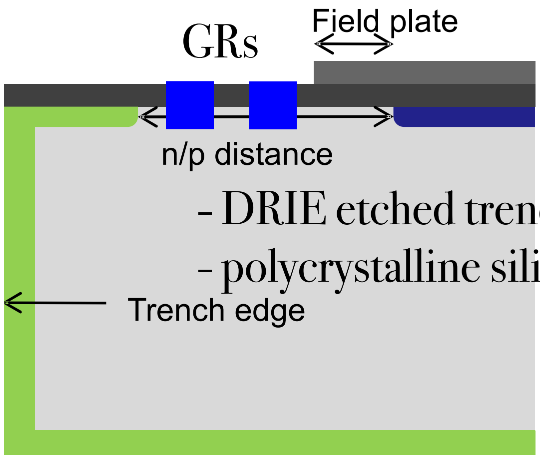

- DRIE etched trench with p+ doping
- polycrystalline silicon trench filling

Design – almost done!

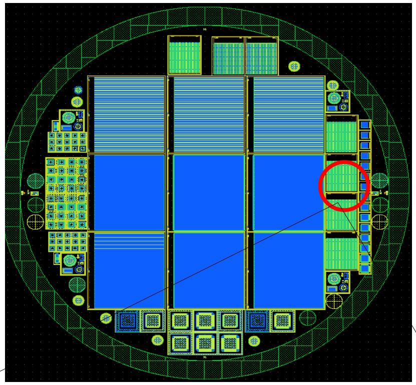

On 4 inch wafer:

→ 9 FEI4
→ 7 FEI3
→ Test structures (diodes, …)

Narrow gap – no GRs

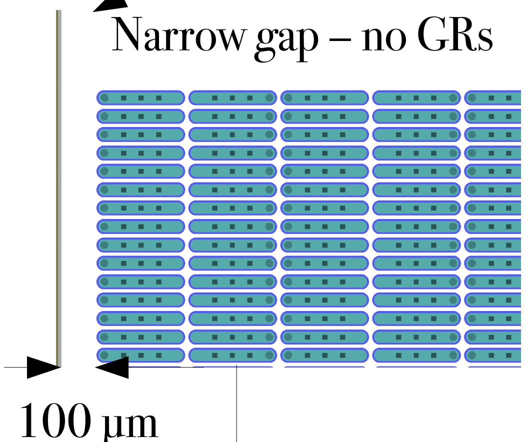

Wide gap – 3 GRs

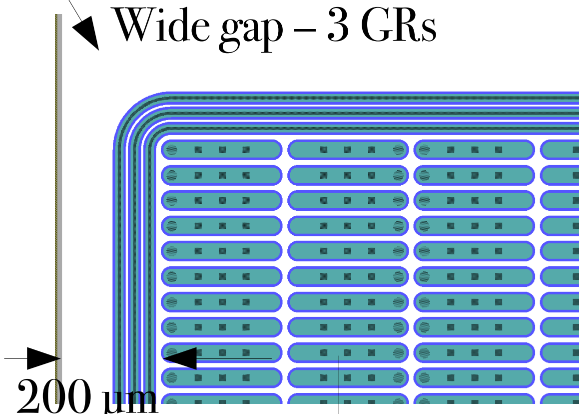

Trench defintion and etching

- Aspect Ratio **1/20**
- Deep etching (200-230 µm)

Trench filling

- Trench width 8-12 µm

Further trench optimization

Trying to reduce trench to less than 10 µm

→Easier to fill the trench

4.5 µm wide

220 µm deep

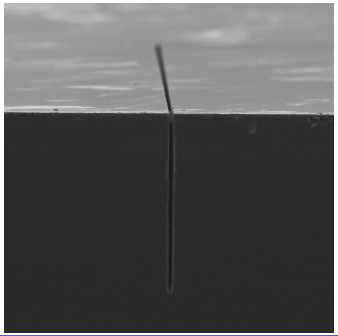

Potential maps @ 100 V

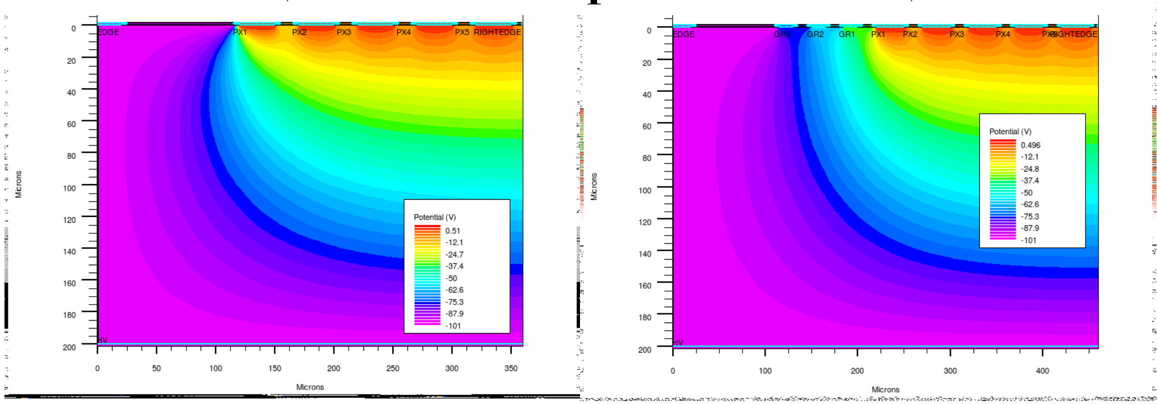

DRIE active EDGE plans

1) Final layout: by this week
2) Masks ready by mid-February
3) Then 4 months for processing
4) Late June: start to test in lab first devices
5) July: irradiations
6) August: bump bonding
7) Late August/September: test on irradiated devices
8) October/November: beam test!

Passivated trench

➔ Need to control potential drop towards the cut edge

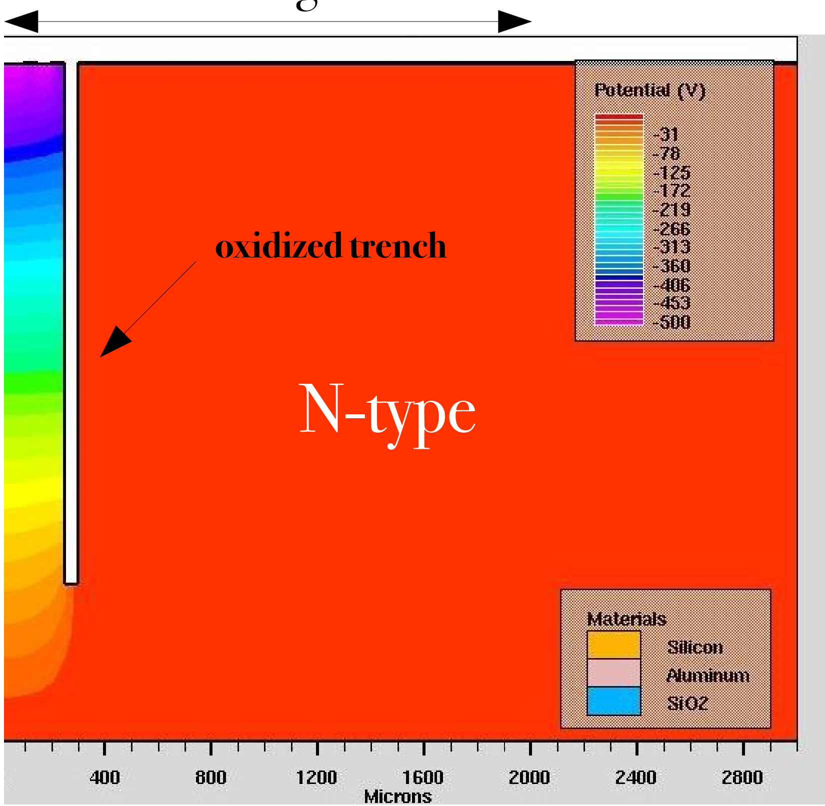

A passivated trench with a thermally grown oxide (**positive** charge density 10^{11} cm^{-2}) trench will lead to:

- ✓ control potential drop toward the cut edge,
- ✓ protection from saw cut edge.

➔ Scribe + nitride/oxide deposit approach too

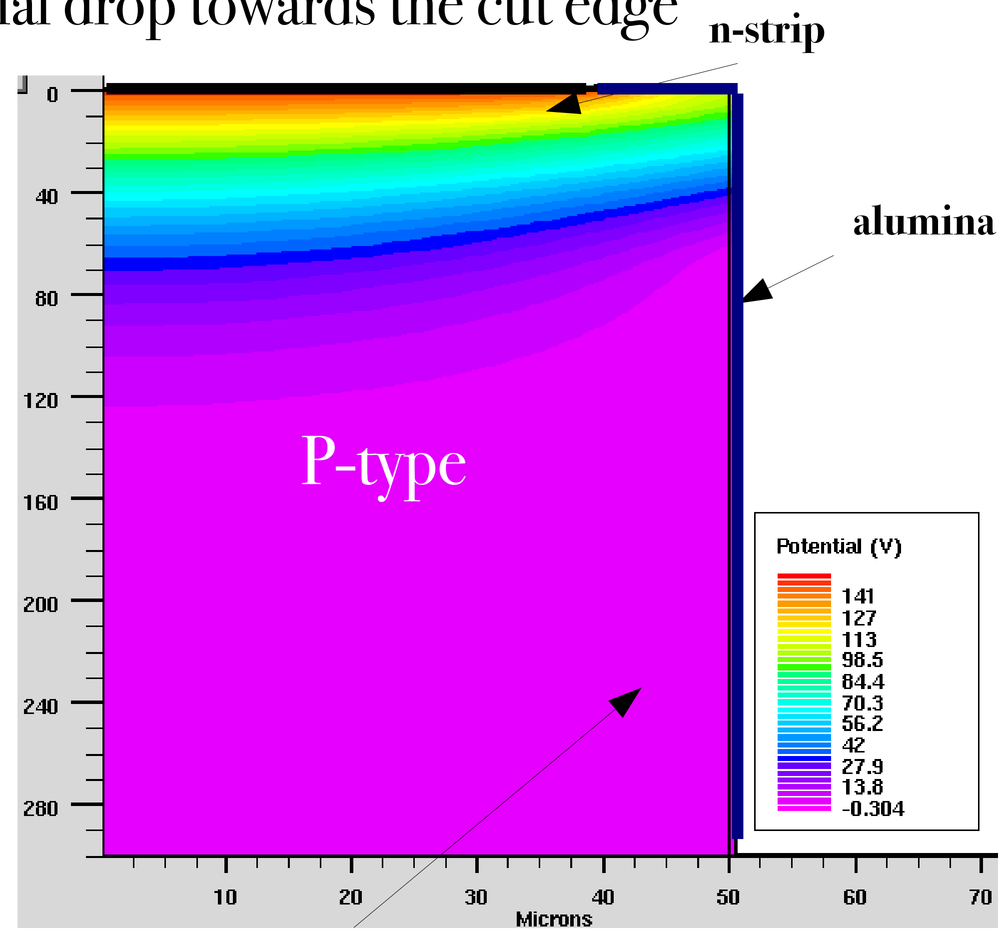

Negative charge ($-1E11$ cm^{-2})

Alumina deposition by ALD

- ✓ Partially controlled potential drop towards the cut edge

➔ The more charge, the better

P-type passivated trench

Examples of Processed Devices

Device A

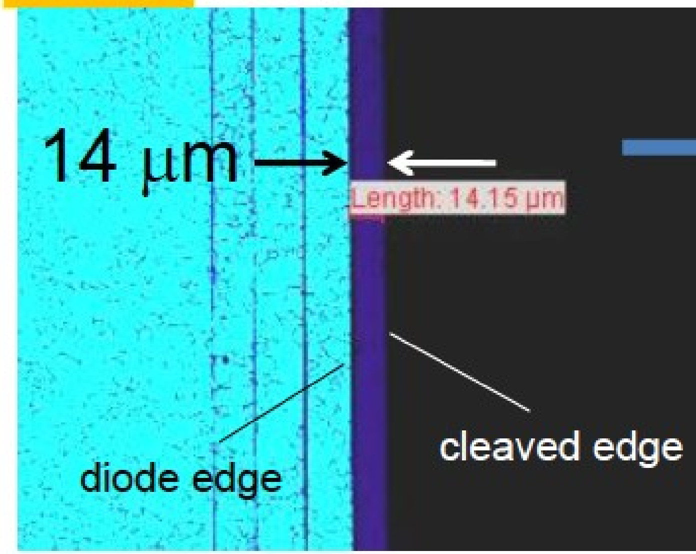

Device B

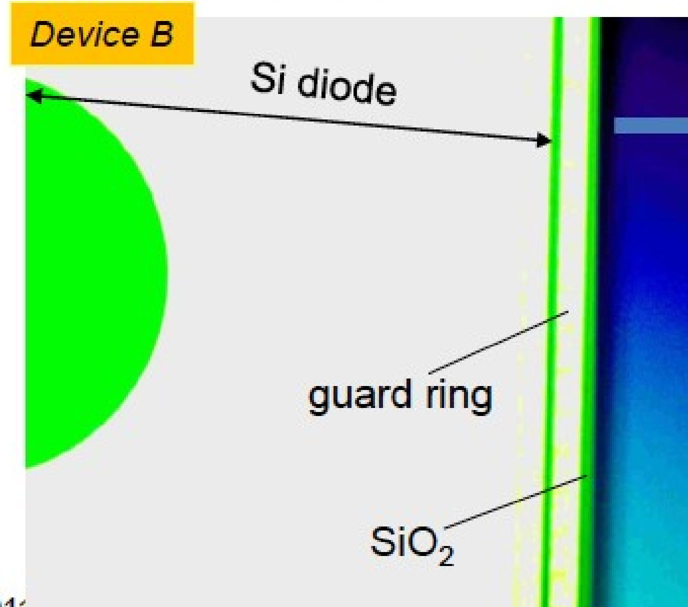

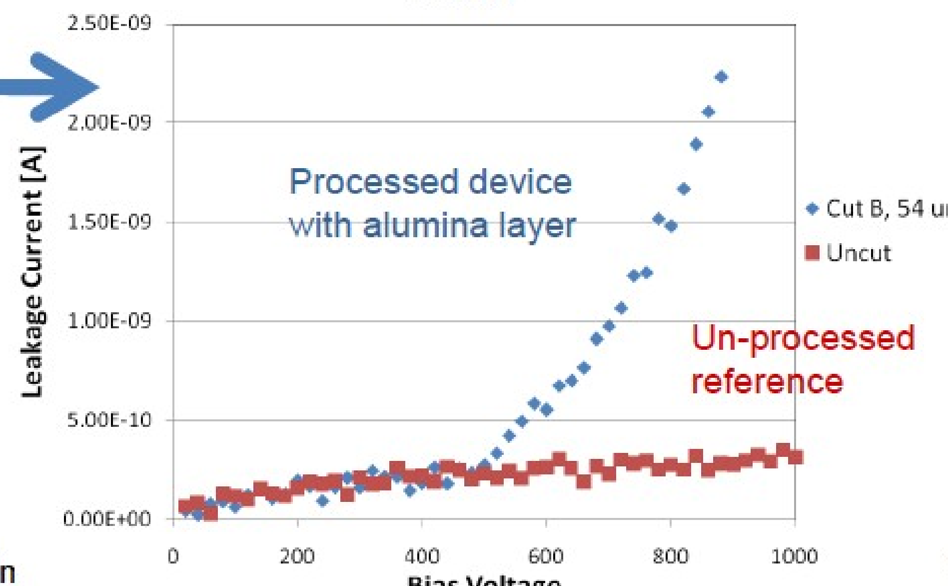

201… UCSC Slin… 3

CONCLUSIONS

Conclusions & Outlook

- A major upgrade of LHC will turn it into a High Luminosity machine
- Foreseen instant and integrated luminosities translate into high occupancies and irradiation fluences for the future ATLAS tracker
- Planar Pixel Sensors Upgrade is investigating the planar technology option
- The PPS group proved radiation hardness of n-&p-type bulk material for a fluence of 5×10^{15} n_{eq}/cm^2 and showed promising results for $\mathcal{O}(10^{16}$ $n_{eq}/cm^2)$
- Dead-area reduction is addressed by means of slim/active edge
- New designs, for both n- & p-type material, including thin bulk, are being studied
- More beamtests will help in realizing the future ATLAS pixel system

The ATLAS PPS Project

- CERN: D. Dobos, C. Gallrapp, B. Di Girolamo, D. Muenstermann, H. Pernegger, S. Roe
- AS CR, Prague (Czech Rep.) : V. Vrba, P. Sicho, J. Popule, M. Tomasek, L. Tomasek, J. Stastny, M. Marcisovsky, M. Havranek, J. Bohm, Z. Janoska, M. Hejtmanek
- LAL Orsay (France): M. Benoit, N. Dinu, D. Fournier, J. Idarraga, A. Lounis
- LPNHE / Paris VI (France): M. Bomben, G. Calderini, J. Chauveau, G. Marchiori, P. Schwemling
- University of Bonn (Germany): M. Barbero, F. Hügging, H. Krüger, N. Wermes
- HU Berlin (Germany): H. Lacker
- DESY (Germany): C. Hengler, I. M. Gregor, U. Husemann, V. Libov, I. Rubinsky
- TU Dortmund (Germany): S. Altenheiner, C. Gößling, J. Jentzsch, T. Lapsien, R. Klingenberg, A. Rummler, G. Troska, T. Wittig, R. Wunstorf
- University of Goettingen (Germany): J. Grosse-Knetter, M. George, A. Quadt, J. Weingarten
- MPP und HLL Munich (Germany): L. Andricek , M. Beimforde, A. Macchiolo, H.-G. Moser, R. Nisius, R. Richter, P. Weigell
- Università degli Studi di Udine – INFN (Italy): D. Cauz, M. Cobal, C. del Papa, D. Esseni, M. P. Giordani, P. Palestri, G. Pauletta, L. Selmi
- KEK (Japan): Y. Unno, S. Terada, Y. Ikegami, Y. Takubo
- IFAE-CNM, Barcelona (Spain): M. Cavalli, S. Grinstein, Korolkov, M. Lozano, C. Padilla, G. Pellegrini, S. Tsiskaridze
- University of Liverpool (UK): T. Affolder, P. Allport, G. Casse, T. Greenshaw, I. Tsurin
- UC Berkeley/LBNL (USA): M. Battaglia, T. Kim, S. Zalusky
- UNM, Albuquerque (USA): I. Gorelov, M. Hoeferkamp, S. Seidel,K. Toms
- UCSC, Santa Cruz (USA): V. Fadeyev, A. Grillo, J. Nielsen, H. Sadrozinski, B. Schumm, A. Seiden

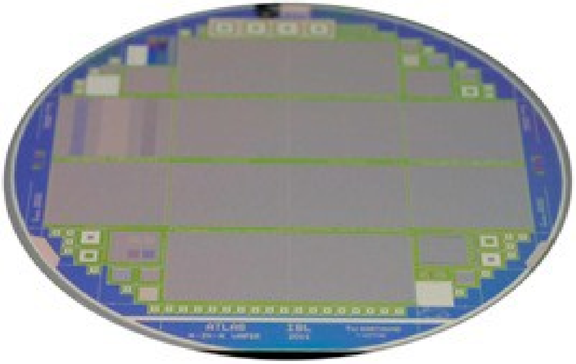

BACKUP

LHC main figures

Circumference (km)	26.7	100-150m underground
Number of superconducting twin-bore Dipoles	1232	Cable Nb-Ti, cold mass 37million kg
Length of Dipole (m)	14.3	
Dipole Field Strength (Tesla)	8.4	Results from the high beam energy needed
Operating Temperature (K) (cryogenics system)	1.9	Superconducting magnets needed for the high magnetic field Super-fluid helium
Current in dipole sc coils (A)	13000	Results from the high magnetic field 1ppm resolution
Beam Intensity (A)	0.5	$2.2.10^{-6}$ loss causes quench
Beam Stored Energy (MJoules)	362	Results from high beam energy and high beam current 1MJ melts 1.5kg Cu
Magnet Stored Energy (MJoules)/octant	1100	Results from the high magnetic field
Sector Powering Circuit	8	1612 different electrical circuits

High luminosity implications

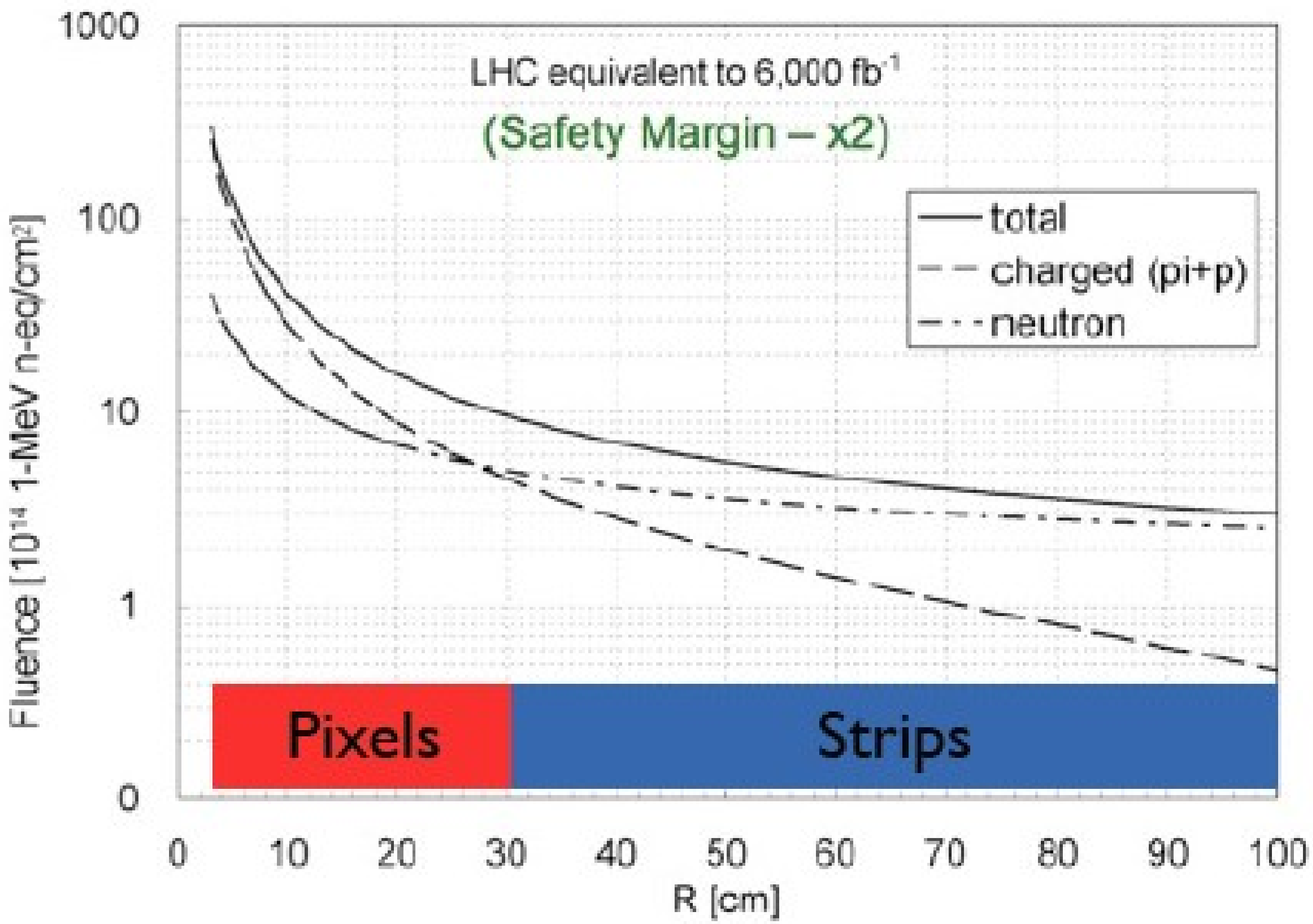

- fluences for the innermost pixel layer: **$1.5 \times 10^{16}\ n_{eq}/cm^2$ (3 ab^{-1})**
- **Radiation hard components**

IBL - layout

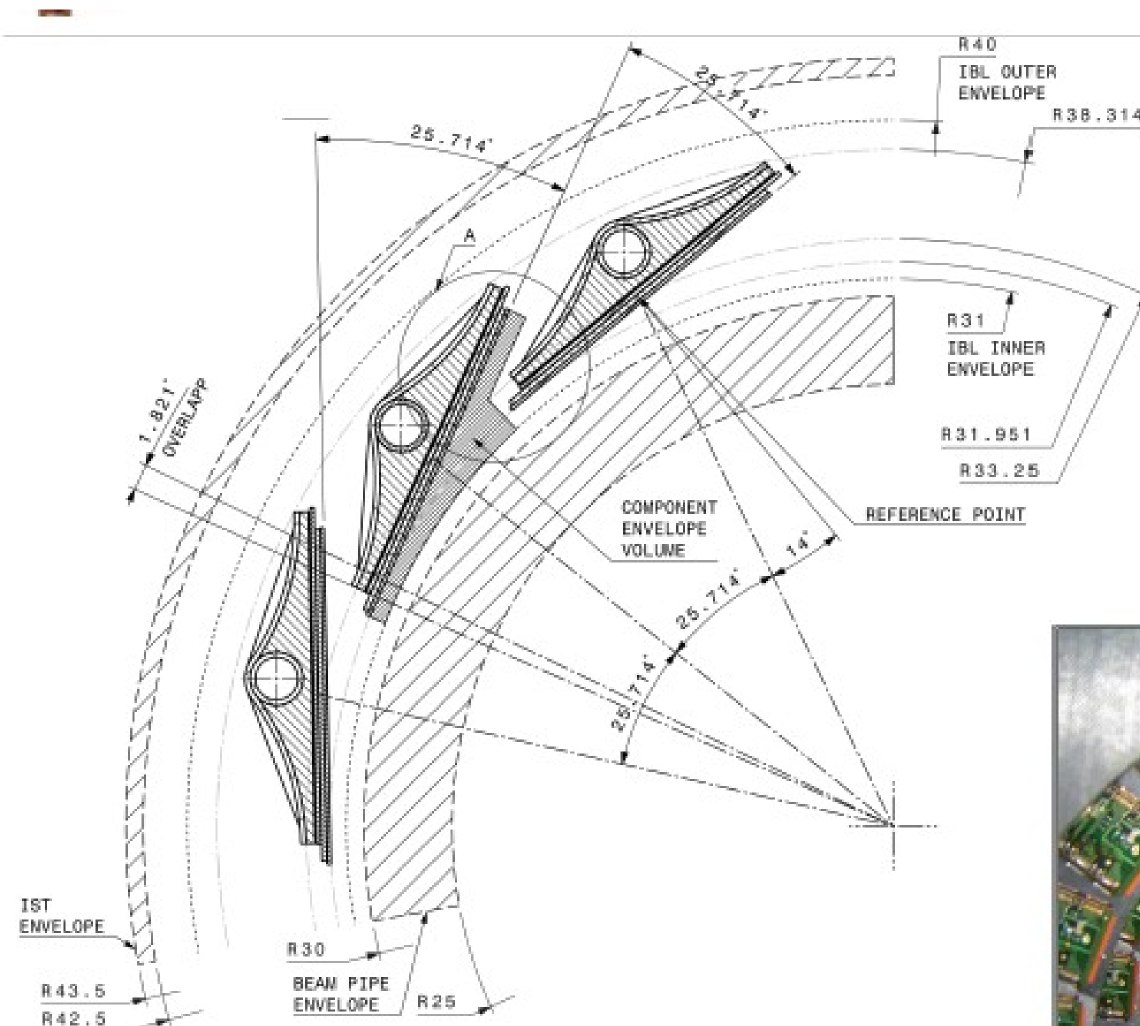

- *Beam-pipe reduction:*
  - Inner R: 29 → 25 mm
- *Very tight clearance:*
  - "Hermetic" to straight tracks in Φ (1.8º overlap)
  - No overlap in Z: minimize gap between sensor active area.
  - Coverage in η (2σ-vertex spread): 2.6
- *Material budget:*
  - Stave, el.serv. Module: 1.16 % X_0
  - IBL Sup.Tube (IST): 0.28 % X_0

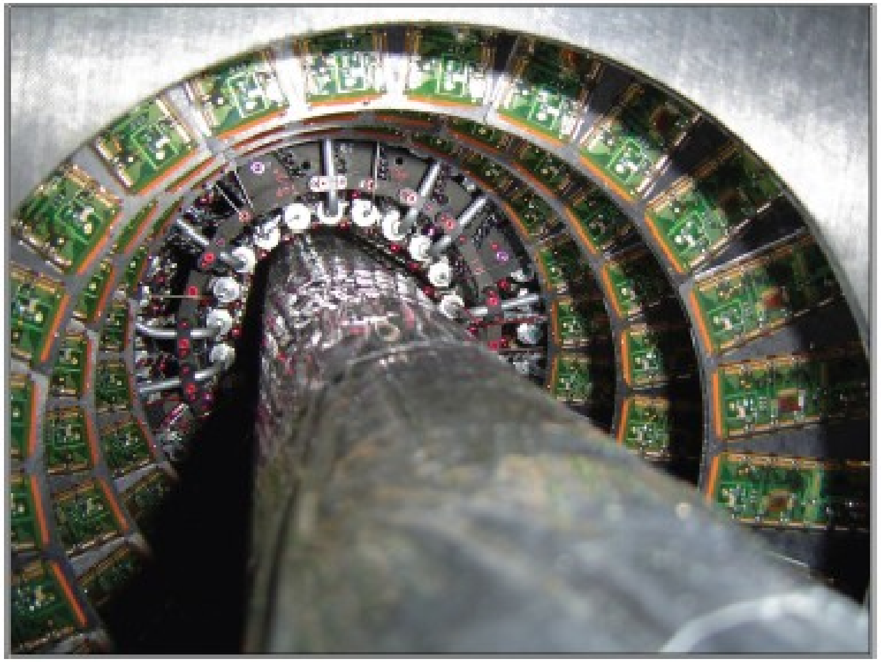

- *Beam-pipe (BP) extracted by cutting the flange on one side and sliding (guiding tube inside).*
- *IBL Support Tube (IST) inserted.*
- *IBL with smaller BP inserted in the IST*

Insertable B-Layer: Motivations

✓ Motivations for a 4^{th} low radius layer in the Pixel Detector

- Luminosity pileup
  - FE-I3 has 5% inefficiency at the B-layer occupancy for $2.2x10^{34}cm^{-2}s^{-1}$
- IBL improves tracking, vertexing and b-tagging for high pileup and recovers eventual failures in present Pixel detector.
  - Today the B-layer has 3.1% of inefficiency.

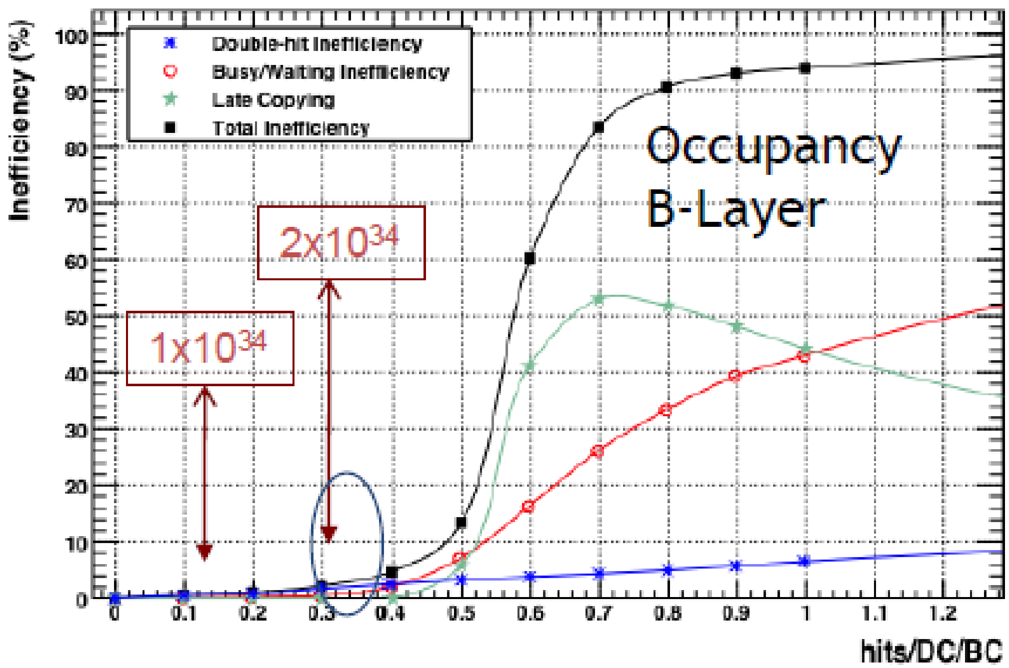

- Radiation damage
  - Degradation of the existing B-Layer reduce detector efficiency after 300-400 fb^{-1}. Not an issue as forecast for 2021 is ~ 330 fb^{-1}
- It serves also as a technology step towards HL-LHC.
- IBL Installation foreseen in 2013, during LHC first shutdown.

IBL performance

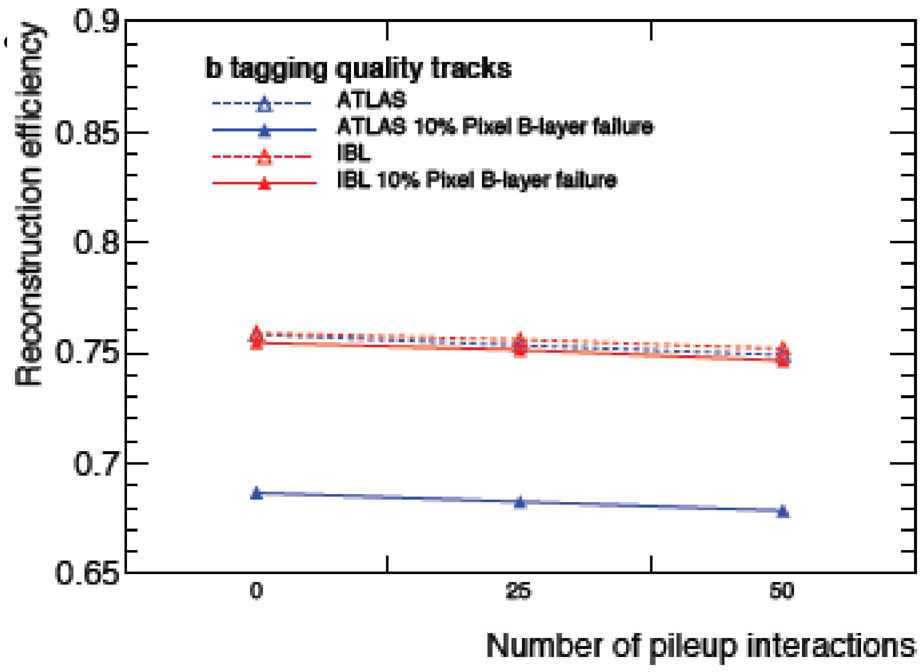

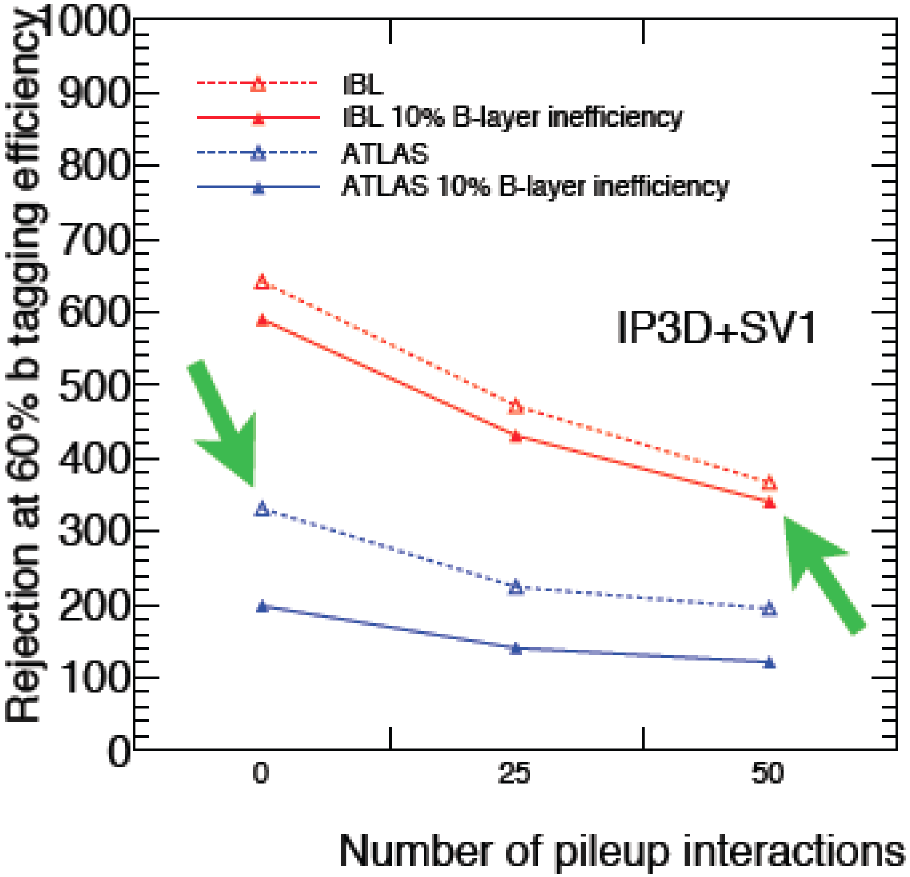

In a scenario with a 10% cluster inefficiency in the actual B-layer, the IBL recovers tracking efficiency and impact resolution

- Only minor effect on b-tagging performances
- Performing better than ATLAS w/o defects and pileup!

N-side read-out can make planar segmented Si detectors suitable for tracking in extreme (SLHC levels: 1-2x10^{16} cm^{-2}) radiation environments.

Schematic changes of Electric field after irradiation

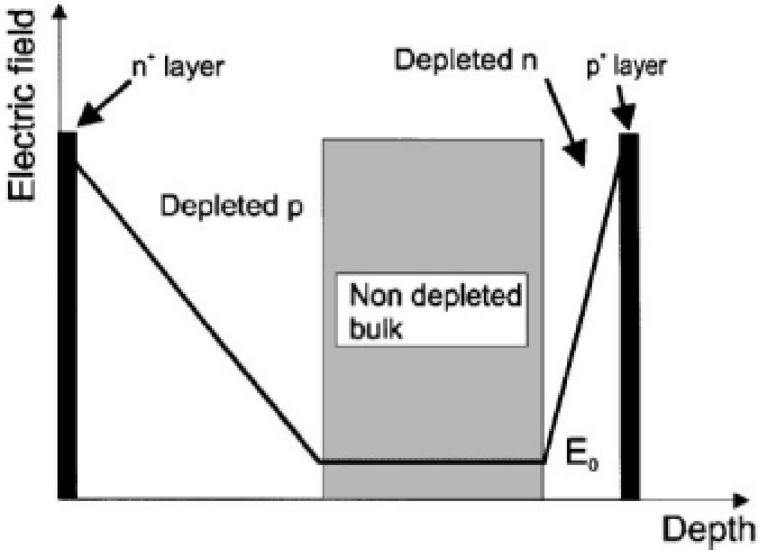

Effect of trapping on the Charge Collection Efficiency (CCE)

$$Q_{tc} \cong Q_0 \exp(-t_c/\tau_{tr}),\ 1/\tau_{tr} = \beta\Phi.$$

Collecting electrons provide a sensitive advantage with respect to holes due to a much shorter t_c. P-type detectors are the most natural solution for *e* collection on the segmented side.

N-side read out to keep lower t_c

Effect of trapping on the Charge Collection Distance

$$Q_{tc} \cong Q_0 \exp(-t_c/\tau_{tr}),\ 1/\tau_{tr} = \beta\Phi.$$

$$v_{sat,e} \times \tau_{tr} = \lambda_{av}$$

$$\beta_e = 4.2E{-}16\ \mathrm{cm^{-2}/ns}$$

$$\beta_h = 6.1E{-}16\ \mathrm{cm^{-2}/ns}$$

G. Kramberger et al., NIMA 476(2002), 645-651.

After heavy irradiation the charge collection distance (CCD) of thin detectors should have a similar (better?) charge collection efficiency (CCE) as thicker ones.

$$\lambda_{Max,n}\ (\Phi=1e14) \cong 2400\mu m$$

$$\lambda_{Max,n}\ (\Phi=1e16) \cong 24\mu m$$

$$\lambda_{Max,p}\ (\Phi=1e14) \cong 1600\mu m$$

$$\lambda_{Max,p}\ (\Phi=1e16) \cong 16\mu m$$

The reverse current is proportional to the depleted volume in irradiated detectors. Do thin sensors offer an advantage in term of reduced reverse current compared to thicker ones (this aspect is particularly important for the inner layer detectors of SLHC, where significant contribution to power consuption is expected from the sensors themselves)?

N-in-p tuning

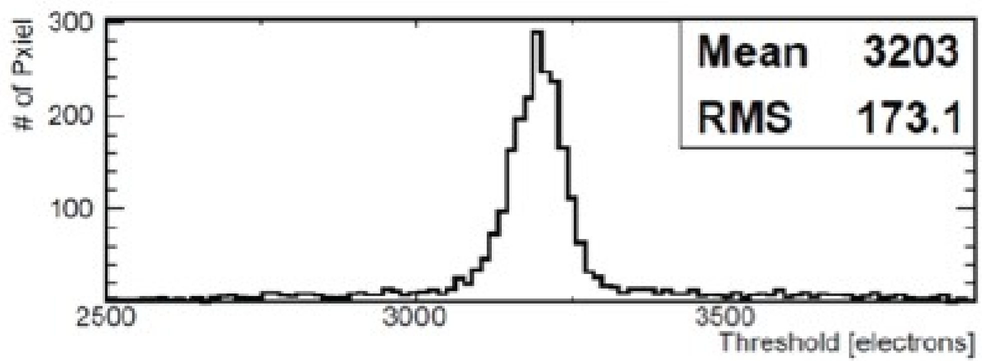

$5 \cdot 10^{15}\ n_{eq}cm^{-2}$

V_{bias}=1kV

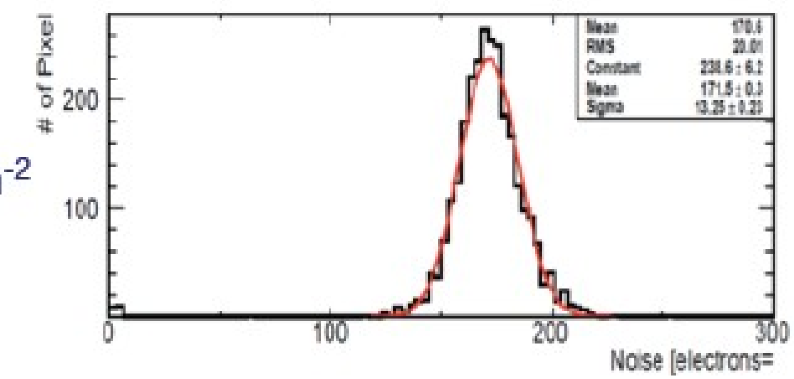

Eudet telescope

- CMOS 0.35 µm
- Pixel size: 18.4x18.4 µm^2
- Rolling shutter mode
  - at 80 MHz → 112.5 µs per frame
  - no deadtime, continues readout
  - digital (binary) readout
- In pixel amplification
- 1 discriminator per column with
  - Offset compensation
  - Correlated Double Sampling
- Built-in data sparsification

- Current version of Mimosa26:
  - High resistivity epitaxial
  - Backthinned down to 50 µm